



UNIVERSITY
OF TRENTO

DIPARTIMENTO DI INGEGNERIA E SCIENZA DELL'INFORMAZIONE

38123 Povo – Trento (Italy), Via Sommarive 14
<http://www.disi.unitn.it>

BAYESIANCOMPRESSIVE SAMPLING FOR PATTERN
SYNTHESISWITHMAXIMALLY SPARSE NON-UNIFORM LINEAR
ARRAYS

G. Oliveri, and A. Massa

January 2011

Technical Report # DISI-11-103

Bayesian Compressive Sampling for Pattern Synthesis with Maximally Sparse Non-Uniform Linear Arrays

G. Oliveri, *Member, IEEE*, and A. Massa, *Member, IEEE*

ELEDIA Research Group

Department of Information Engineering and Computer Science,

University of Trento, Via Sommarive 14, 38050 Trento - Italy

Tel. +39 0461 882057, Fax +39 0461 882093

E-mail: *andrea.massa@ing.unitn.it, giacomo.oliveri@disi.unitn.it*

Web-site: *http://www.eledia.ing.unitn.it*

Bayesian Compressive Sampling for Pattern Synthesis with Maximally Sparse Non-Uniform Linear Arrays

G. Oliveri and A. Massa

Abstract

This paper introduces a numerically-efficient technique based on the Bayesian Compressive Sampling (*BCS*) for the design of maximally-sparse linear arrays. The method is based on a probabilistic formulation of the array synthesis and it exploits a fast relevance vector machine (*RVM*) for the problem solution. The proposed approach allows the design of linear arrangements fitting desired power patterns with a reduced number of non-uniformly spaced active elements. The numerical validation assesses the effectiveness and computational efficiency of the proposed approach as a suitable complement to existing state-of-the-art techniques for the design of sparse arrays.

Key words: Array synthesis, sparse arrays, bayesian compressive sampling, relevance vector machine.

1 Introduction

Synthesizing antenna arrays with a minimum number of elements is a problem of high importance in those applications (e.g., satellite communications, radars, biomedical imaging, acoustics, and remote sensing) where the weight, the consumption, and the hardware/software complexity of the radiating device have a strong impact on the whole cost of the overall system [1][2].

Non-uniform arrangements have potential advantages with respect to uniform layouts [3] such as (a) significantly increased resolution (i.e, decreased mainlobe width) [4], (b) sidelobe level control/reduction [5], and (c) enhanced efficiency in dealing with physically-constrained geometries (e.g., conformal architectures) [6]. However, sparsening array elements has the main drawback of reducing the control of the beam shape [1]-[7] and several approaches for the design and optimization of sparse arrangements have been proposed in the last 50 years [1]-[30] to properly address such an issue.

Dealing with beam shape control, two different problems are usually considered in the state-of-the-art literature [20]: (I) the minimization of the peak sidelobe level (*PSL*) by determining a fixed set of N element positions over an aperture and sometimes the corresponding weights; (II) the synthesis of a maximally-sparse array⁽¹⁾ radiating a desired pattern. A wide set of methods concerned with *Problem I* [2] has been investigated including random approaches [11][15], dynamic programming [12], *FIR*-filter design [16], stochastic optimization methods [17][18][20][24][27][28], analytical techniques [22][30], and hybrid algorithms [25][29], as well. On the contrary, *Problem II* has received less attention and few methods have been developed [2][3][13][14][19][20][21][23][26]. Because of the limitations of available computers, first attempts relied on techniques requiring as few computational resources as possible such as the steepest descent method [13] and the iterative least-square technique [14]. However, those approaches have strong limitations as, for example, the need to *a-priori* know the number of active elements of the array and the aperture size [13][14]. In order to overcome these drawbacks, a technique exploiting the simplex search was developed in [3] to find the sparsest array match-

⁽¹⁾ An array with the minimum number of active elements, P , over a lattice (regular or irregular) of N positions.

ing a given reference pattern. Moreover, a mixed linear programming approach was introduced in [19] with the same aim. Further developments ranging from a recursive inversion algorithm based on the Legendre transform [21][26] up to the use of a stochastic optimizer based on the simulated annealing technique [20] or a generalized Gaussian quadrature approach [23] have been successively analyzed. More recently, *Problem II* has been solved by means of an innovative technique based on the Matrix Pencil Method (*MPM*) [7]. Thanks to its efficiency, the *MPM* generally outperforms other synthesis techniques in terms of convergence speed and array performances [7]. Despite its effectiveness, such an approach presents some limitations:

1. the locations $d_p, p = 1, \dots, P$, of the P active elements of the array are proportional to the complex values of the non-zero roots of the generalized eigenvalue problem described in [7]. Consequently, *unphysical* complex solutions (i.e., $d_p \in \mathbb{C}$) can be generated [7] and an approximation [i.e., $d_p^{MPM} = \Re(d_p)$] is required (p. 2957 - [7]) whose impact on the array performances cannot be *a-priori* estimated nor neglected;
2. no requirements on the element positions [7] can be stated. Thus, no geometrical regularity or user-desired geometric features on the synthesized array can be *a-priori* enforced;
3. the method may fail in synthesizing/matching shaped beam patterns because of the imaginary parts of $d_p, p = 1, \dots, P$ are not usually negligible (p. 2958 - [7]).

This paper is aimed at proposing an innovative, flexible, and computationally-efficient complement to the existing synthesis methods that solve *Problem II*. The method, based on the Bayesian Compressive Sampling (*BCS*) [31], is devoted to find the maximally-sparse array with the highest *a-posteriori* probability to match a user-defined reference pattern. Towards this end, an efficient *BCS* solver exploiting a fast relevance vector machine (*RVM*) algorithm [31] is adopted.

The outline of the paper is as follows. Section 2 is aimed at mathematically formulating the synthesis problem and describing an algorithm for minimizing a suitable cost function that depends on the degree of sparseness of the array and the mismatch between the desired power pattern and the actual one. Section 3 provides a selected set of numerical results to validate

the proposed approach as well as to compare its performances with state-of-the-art techniques. Finally, some conclusions are drawn (Sect. 4).

2 Mathematical Formulation

2.1 BCS Formulation

Let us consider a symmetric linear arrangement of $M = 2 \times N - \chi$ ($\chi = 0$ if an even number of elements is at hand, $\chi = 1$ otherwise) isotropic elements, $w_n \in \mathbb{R}$ being the real excitation of the n -th element pair ($n = 1, \dots, N$). The synthesis problem is that of finding the set of array weights such that (a) the radiated pattern is sufficiently close to a given reference one, $E_{REF}(u)$, and (b) the number P of *active* (i.e., $w_n = w_{-n} = \delta_{np}w_p$, $p = 1, \dots, P$, δ_{np} being the Kronecker function) array elements is as small as possible [3]. Towards this end, the *BCS* formulation is considered and similarly to [3] the following assumptions are taken into account: (a) the reference pattern is approximated in an arbitrary set of K angular positions u_k , $k = 1, \dots, K$, within the visible range ($u_k \in [-1, 1]$); (b) the set of P active positions are constrained to a large, but finite, user-chosen set of M (i.e., $M \gg P$) candidate locations not necessarily belonging to a regular lattice. Mathematically, the problem can be formulated as follows

Synthesis Problem - Given a set of K samples of the reference pattern, $\mathbf{E}_{REF} \in \mathbb{R}^K$, and a fidelity factor ε find the set of array weights, \mathbf{w} , which is maximally sparse subject to $\|\mathbf{E}_{REF} - \mathbf{E}\|^2 \leq \varepsilon$

where $\|\cdot\|$ is the ℓ_2 -norm, $\mathbf{E}_{REF} \triangleq [E_{REF}(u_1), \dots, E_{REF}(u_K)]^H$, $\mathbf{w} \triangleq [w_1, \dots, w_N]^H$, $\mathbf{E} \triangleq [E(u_1), \dots, E(u_K)]^H$ whose k -th entry is given by $E(u_k) = \sum_{n=1}^N \nu_n w_n \cos\left[\frac{2\pi d_n u_k}{\lambda}\right]$, λ being the wavelength, d_n the distance of the n -th location from the array center ($d_1 = 0$ if $\chi = 1$), and ν_n is the Neumann's number [9] defined as $\nu_n = 2 - \chi$ if $n = 1$, and $\nu_n = 2$ otherwise.

The synthesized pattern samples \mathbf{E} can be then expressed as

$$\mathbf{E} = \Psi \mathbf{w} \quad (1)$$

where $\Psi \in R^{K \times N}$ and its (k, n) -th element is given by $\psi(k, n) = \nu_n \cos\left[\frac{2\pi d_n u_k}{\lambda}\right]$.

To recast the problem at hand as a *BCS* problem, the following three steps are necessary. Let us first rewrite the ℓ_2 -norm constraint ($\|\mathbf{E}_{REF} - \mathbf{E}\|^2 \leq \varepsilon$) as⁽²⁾ [34]

$$\mathbf{E}_{REF} - \Psi \mathbf{w} = \mathbf{e} \quad (2)$$

where $\mathbf{e} = [e_1, \dots, e_K]^T$ is a zero mean Gaussian error vector [31][33][34] with an user-defined variance σ^2 proportional to the mismatching with the reference pattern (i.e., $\sigma^2 \propto \varepsilon$). Then, let us model \mathbf{E}_{REF} through a Gaussian likelihood model

$$p(\mathbf{E}_{REF} | [\mathbf{w}, \sigma^2]) = \frac{1}{(2\pi\sigma^2)^{\frac{K}{2}}} \exp\left(-\frac{1}{2\sigma^2} \|\mathbf{E}_{REF} - \Psi \mathbf{w}\|^2\right) \quad (3)$$

to recast the original problem as the following linear regression one with sparseness constraints (*LRSC*)

LRSC Problem - Given $\mathbf{E}_{REF} \in \mathbb{R}^K$ find \mathbf{w} and σ^2 which maximize the a-posteriori probability $p(\mathbf{w}, \sigma^2 | \mathbf{E}_{REF})$ subject to the constraint that \mathbf{w} is maximally-sparse

Finally, the sparseness of \mathbf{w} [33][34] is enforced. As regards the Bayesian formulation, such a task is accomplished by introducing a sparseness prior⁽³⁾ over \mathbf{w} [31]. Hereinafter, the Gaussian hierarchical prior [32][33][34] is invoked

$$p(\mathbf{w} | \mathbf{a}) = \frac{\prod_{n=1}^N \sqrt{a_n} \exp\left(-\frac{a_n w_n^2}{2}\right)}{(2\pi)^{\frac{N}{2}}} \quad (4)$$

where $\mathbf{a} \triangleq [a_1, \dots, a_N]$ and a_n ($n = 1, \dots, N$) is the n -th independent hyperparameter controlling the strength of the prior over w_n [32]. To fully specify (4), the hyperpriors over \mathbf{a} [i.e., $p(\mathbf{a})$] and σ^2 [i.e., $p\left(\frac{1}{\sigma^2}\right)$] have to be defined. The Gamma distributions are here considered [32]

$$p(\mathbf{a}) = \prod_{n=1}^N G(a_n | \alpha_1, \alpha_2) \quad (5)$$

and

⁽²⁾ It is worth pointing out that Eq. (2) and the ℓ_2 -norm constraint are mathematically equivalent [34].

⁽³⁾ In Bayesian inference, a *prior* represents the *a-priori* knowledge about an unknown quantity in probabilistic terms.

$$p\left(\frac{1}{\sigma^2}\right) = G\left(\frac{1}{\sigma^2} \mid \alpha_3, \alpha_4\right) \quad (6)$$

where α_i ($i = 1, \dots, 4$) is the i -th *scale prior*, $G(a_n \mid \alpha_1, \alpha_2) \triangleq \frac{\alpha_2^{\alpha_1} a_n^{\alpha_1-1} e^{-\alpha_2 a}}{\Gamma(\alpha_1)}$, and $\Gamma(\alpha_1) \triangleq \int_0^\infty t^{\alpha_1-1} e^{-t} dt$ is the gamma function [32]. Thanks to (4), (5), and (6), the original synthesis problem can be finally formulated as

BCS Problem - Given $\mathbf{E}_{REF} \in \mathbb{R}^K$, find \mathbf{w}_{BCS} , \mathbf{a}_{BCS} , and σ_{BCS}^2 which maximize $p([\mathbf{w}, \mathbf{a}, \sigma^2] \mid \mathbf{E}_{REF})$.

2.2 BCS Solver - The RVM Procedure

In order to solve the *BCS Problem* by determining the unknown parameters \mathbf{w}_{BCS} , \mathbf{a}_{BCS} , and σ_{BCS}^2 , the *RVM* method [32][31] is applied. Towards this end, let us consider that the posterior over all unknowns can be expressed as

$$p([\mathbf{w}, \mathbf{a}, \sigma^2] \mid \mathbf{E}_{REF}) = p(\mathbf{w} \mid [\mathbf{E}_{REF}, \mathbf{a}, \sigma^2]) p([\mathbf{a}, \sigma^2] \mid \mathbf{E}_{REF}). \quad (7)$$

Moreover, because of (3) and (4), the posterior distribution over \mathbf{w}

$$p(\mathbf{w} \mid [\mathbf{E}_{REF}, \mathbf{a}, \sigma^2]) = \frac{p(\mathbf{E}_{REF} \mid [\mathbf{w}, \sigma^2]) p(\mathbf{w} \mid \mathbf{a})}{p(\mathbf{E}_{REF} \mid [\mathbf{a}, \sigma^2])} \quad (8)$$

turns out to be equal to the following multivariate Gaussian distribution [34]

$$p(\mathbf{w} \mid [\mathbf{E}_{REF}, \mathbf{a}, \sigma^2]) = \frac{1}{(2\pi)^{\frac{N+1}{2}} \sqrt{\det(\Sigma)}} \exp\left\{-\frac{(\mathbf{w} - \mu)^H (\Sigma)^{-1} (\mathbf{w} - \mu)}{2}\right\} \quad (9)$$

where the posterior mean and the covariance are given by $\mu = \frac{\Sigma \Psi^H \mathbf{E}_{REF}}{\sigma^2}$ and $\Sigma = \left(\frac{\Psi^T \Psi}{\sigma^2} + A\right)^{-1}$, respectively, being $A \triangleq \text{diag}(a_1, \dots, a_N)$.

As for the second term on the right-hand side of (7), the delta-function approximation is used [32] to model the hyperparameter posterior

$$p([\mathbf{a}, \sigma^2] \mid \mathbf{E}_{REF}) \approx \delta(\mathbf{a}_{BCS}, \sigma_{BCS}^2) \quad (10)$$

where \mathbf{a}_{BCS} and σ_{BCS}^2 are the most probable values, $(\mathbf{a}_{BCS}, \sigma_{BCS}^2) = \arg \max_{\mathbf{a}, \sigma^2} \{p([\mathbf{a}, \sigma^2] | \mathbf{E}_{REF})\}$, also called hyperparameter posterior *modes*. In order to determine their values, let us consider that

$$p([\mathbf{a}, \sigma^2] | \mathbf{E}_{REF}) \propto p(\mathbf{E}_{REF} | [\mathbf{a}, \sigma^2]) p(\mathbf{a}) p(\sigma^2) \quad (11)$$

and let us assume uniform scale priors. Then, $p(\sigma^2)$ and $p(\mathbf{a})$ become constant values [32] and the maximization of (11) is equivalent to maximize the term $p(\mathbf{E}_{REF} | \mathbf{a}, \sigma^2)$, whose logarithm is given by [32]

$$\mathcal{L}(\mathbf{a}, \sigma^2) \triangleq \log [p(\mathbf{E}_{REF} | \mathbf{a}, \sigma^2)] = -\frac{1}{2} [N \log 2\pi + \log |C| + \mathbf{E}_{REF}^H C^{-1} \mathbf{E}_{REF}] \quad (12)$$

where $C = \sigma^2 I + \Psi A^{-1} \Psi^T$. It is worthwhile to point out that it is not possible to perform the maximization of the ‘‘marginal likelihood’’ (12) in an exact fashion, but a *type-II maximum likelihood* procedure [34] can be profitably exploited for determining an iterative re-estimation of $(\mathbf{a}_{BCS}, \sigma_{BCS}^2)$. Such a technique, whose Matlab implementation is available in [35], is summarized in the Appendix.

Finally, by substituting (9) and (10) in (7), one obtains that

$$p([\mathbf{w}, \mathbf{a}, \sigma^2] | \mathbf{E}_{REF}) \approx p(\mathbf{w} | [\mathbf{E}_{REF}, \mathbf{a}, \sigma^2]) \Big|_{(\mathbf{a}, \sigma^2) = (\mathbf{a}_{BCS}, \sigma_{BCS}^2)}. \quad (13)$$

The posterior over all unknowns results a multivariate Gaussian function (9) only depending on the unknown set \mathbf{w} once $(\mathbf{a}_{BCS}, \sigma_{BCS}^2)$ have been determined. Therefore, the value of $\mathbf{w}_{BCS} = \arg \max_{\mathbf{w}} \{p([\mathbf{w}, \mathbf{a}, \sigma^2] | \mathbf{E}_{REF})\}$ turns out to be equal to the posterior mean of $p(\mathbf{w} | [\mathbf{E}_{REF}, \mathbf{a}, \sigma^2]) \Big|_{(\mathbf{a}, \sigma^2) = (\mathbf{a}_{BCS}, \sigma_{BCS}^2)}$ given by

$$\mathbf{w}_{BCS} = \mu \Big|_{(\mathbf{a}, \sigma^2) = (\mathbf{a}_{BCS}, \sigma_{BCS}^2)}. \quad (14)$$

2.3 BSC Synthesis Method - Algorithmic Implementation

The algorithmic implementation of the *BCS*-based pattern synthesis consists of the following steps:

1. *Input Phase* - Set the reference pattern $E_{REF}(u)$, the grid of admissible locations (d_n ; $n = 1, \dots, N$), the set of pattern sampling points (u_k ; $k = 1, \dots, K$), the target variance σ^2 of the error term \mathbf{e} , and its *initial estimate* σ_0^2 for the sequential solver of the *RVM* algorithm (see the Appendix);
2. *Matrix Definition* - Fill the entries of the matrices \mathbf{E}_{REF} , Ψ , \mathbf{e} , and $\hat{\mathbf{E}}_{REF} = \mathbf{E}_{REF} + \mathbf{e}$;
3. *Hyperparameter Posterior Modes Estimation* - Find $(\mathbf{a}_{BCS}, \sigma_{BCS}^2)$ by maximizing (12) as described in the Appendix;
4. *Array Weights Estimation* - Find \mathbf{w}_{BCS} by (14);
5. *Output Phase* - Return the estimated array weights, \mathbf{w}_{BCS} , the number of active array elements, $P_{BCS} = -\chi + 2 \|\mathbf{w}_{BCS}\|_0^{(4)}$, and the corresponding hyperparameter modes $(\mathbf{a}_{BCS}, \sigma_{BCS}^2)$.

Starting from an user-required pattern $E_{REF}(u)$ (i.e., its sampled representation \mathbf{E}_{REF}), the control parameters of the synthesis process are the following variables: (a) d_n , $n = 1, \dots, N$; (b) u_k , $k = 1, \dots, K$; (c) σ^2 , and (d) σ_0^2 . Consequently, it is possible to synthesize arbitrary reference patterns specifying the pattern matching accuracy (c) and the sequential solver initialization (d). Moreover, the *BCS* method allows one to enforce pattern constraints within the whole or in a subset of the visible range (b) as well as to set suitable geometrical features of the array arrangement (a).

3 Numerical Analysis and Assessment

This section is devoted to numerically assess potentialities and limitations of the proposed *BCS* approach for the design of sparse linear arrays. The numerical analysis is carried out by considering a set of representative/benchmark reference patterns to evaluate the effectiveness and

⁽⁴⁾In this paper $\|\mathbf{x}\|_0$ is the ℓ_0 -norm of \mathbf{x} (i.e., the number of non-zero elements of \mathbf{x}).

reliability of the *BCS* in approximating a user-desired pattern. In order to evaluate the “degree of optimality” of the array designs, the following metrics and pattern descriptors are used: the matching error ξ defined as⁽⁵⁾

$$\xi \triangleq \frac{\int_0^1 |E_{REF}(u) - E(u)|^2 du}{\int_0^1 |E_{REF}(u)|^2 du}, \quad (15)$$

the aperture length L , the mean inter-element spacing $\Delta L = \frac{L}{P-1}$, and the minimum spacing $\Delta L_{min} = \min_{p=1, \dots, P-1} \{|d_{p+1} - d_p|\}$.

3.1 *BCS* Sensitivity Analysis

As a first numerical experiment, the synthesis of a non-uniform array matching a Dolph-Chebyshev pattern [2] is considered. A broadside Dolph-Chebyshev pattern with $L = 9.5\lambda$ and $PSL = -20$ [dB] is assumed as reference. Let us notice that such a pattern can be synthesized through a uniform array with $P_{UNI} = 20 \frac{\lambda}{2}$ -spaced elements. The *BCS* synthesis has been carried out by sampling $E_{REF}(u)$ at K points ($u_k \in [0, 1]$, $u_k = \frac{k-1}{K-1}$, $k = 1, \dots, K$) and assuming the following grid of admissible locations

$$d_n = \frac{L(n-1)}{2(N-1)}, \quad n = 1, \dots, N. \quad (16)$$

Figure 1(a) describes the *BCS* results by reporting the matching error ξ versus the number of active elements P_{BCS} for different values of the control parameters: $K = \{5, \dots, 25\}$, $\sigma^2 \in [10^{-5}, 1]$, $\sigma_0^2 \in [10^{-5}, 1]$, and $N \in [5, 5 \times 10^4]$. The Pareto front of the solution set in the plane (ξ, P_{BCS}) is indicated, as well. As it can be observed, different *BCS* trade-off solutions are obtained with accuracy and element number in the range $\xi \in [10^{-6}, 2]$ and $P_{BCS} \in [5, 20]$, respectively. By comparing the patterns related to three representative points of the Pareto front (i.e., $P_{BCS} = \{8, 14, 20\}$) with the reference one [Fig. 1(b)], it turns out that the solution with $P_{BCS} = 8$ elements provides a very poor matching ($\xi = 2.91 \times 10^{-1}$), while a reliable reconstruction ($\xi = 0.99 \times 10^{-4}$) is yielded choosing the solution having $P_{BCS} = 14$ [Fig. 1(b)] with a non-negligible saving of array elements with respect to the $\frac{\lambda}{2}$ -spaced uniform array (i.e.,

⁽⁵⁾Only $u \in [0, 1]$ is considered in the definition of ξ for symmetry reasons.

$\frac{P_{BCS}}{P_{UNI}} = 0.7$). As a general by-product, it results that a value of the accuracy index around the threshold $\xi = 10^{-4}$ identifies an optimal trade-off *BCS* solution, whereas lower ξ values usually require more radiating elements [$P_{BCS} = 20$, $\xi = 2.03 \times 10^{-6}$ - Fig. 1(b)] without significant/relevant improvements in the matching of the reference pattern. As regards the resulting layouts, it is worth pointing out that the optimal *BCS* array ($P_{BCS} = 14$) has an aperture and an excitation displacement [Fig. 1(c)] close to those of the uniform array. This proves the effective non-uniform sampling of the ideal current distribution affording $E_{REF}(u)$. Otherwise, different apertures [e.g., $L_{BCS}|_{P=8} = 6.2\lambda$ vs. $L_{BCS}|_{P=14} = 9.5\lambda$] and weights [Fig. 1(c)] are synthesized in correspondence with greater values of ξ . As for the element arrangement, a positive feature of the *BCS* arrays is the enlarged inter-element spacing with respect to the corresponding uniform array [Fig. 1(c)] despite the closely-spaced admissible locations [Eq. (16)].

In order to provide a deeper understanding about the sensitivity of the *BCS* performances on the control parameters, Figures 2 and 3 summarize the results of a comprehensive numerical analysis. More specifically, the matching error has been evaluated as a function of K , or σ_0^2 , or σ^2 , or N by setting the other parameters to the values used to obtain the optimal trade-off with $P_{BCS} = 14$ (i.e., $K = 15$, $\sigma^2 = 10^{-2}$, $\sigma_0^2 = 2.0 \times 10^{-3}$, $N = 501$). For completeness, the behavior of P_{BCS} has been reported, as well. As expected [Fig. 2(a)], the pattern matching improves as the number of samples K of $E_{REF}(u)$ increases. However, ξ does not further decrease beyond a threshold value ($K = 15$) slightly above the Nyquist threshold ($K_{Nyquist} = 11$) even though the corresponding number of array elements P_{BCS} still grows. A sampling value K between $K_{Nyquist}$ and $1.5K_{Nyquist}$ turns out to be a reliable choice as confirmed by the behaviour of the plots of $|E_{BCS}(u) - E_{MPM}(u)|^2$ for $K = \{7, 15, 24\}$ [Fig. 3(a)], as well. Indeed, the lowest value of K gives the poorest fitting [$\xi|_{K=7} = 0.91$ - Fig. 3(a)], while satisfactory reconstructions are obtained when $K > K_{Nyquist}$ ($\xi|_{K=15} = 0.99 \times 10^{-4}$). A further increment of K only marginally enhances the accuracy [$\xi|_{K=24} = 0.98 \times 10^{-4}$ - Fig. 3(a)].

Concerning the sensitivity to σ^2 , the integral error has small variations for $\sigma^2 < 10^{-2}$, while it sharply increases afterwards [Fig. 2(b)] as pointed out by the plots of $|E_{BCS}(u) - E_{REF}(u)|^2$

in correspondence with a set of representative values of σ^2 (i.e., $\sigma^2 = \{10^{-5}, 10^{-2}, 1\}$) [Fig. 3(b)]. More sparse arrays are synthesized in correspondence with larger values of σ^2 at the expense of higher ξ values [Fig. 2(b)]. Good tradeoffs between accuracy and element reduction then arise by setting $\sigma^2 \in [10^{-3}, 10^{-1}]$. Such an outcome indicates that the *BCS* performances are significantly less sensitive to σ^2 than to K . As a matter of fact, a reduction of ξ of about one order in magnitude requires a variation of K of about 10 – 20% [Fig. 2(a)], while the same effect holds true for a variation of σ^2 of more than two orders in magnitude [Fig. 2(b)]. Similar deductions can be drawn from the behaviour of the integral error versus σ_0^2 . Moreover, the matching error increases almost monotonically with σ_0^2 , whereas low P_{BCS} values are obtained within the range $\sigma_0^2 \in [5.0 \times 10^{-4}, 5.0 \times 10^{-2}]$ [Fig. 2(c)]. Such a range can be also assumed as reference guideline since smaller σ_0^2 values only marginally improve the matching accuracy [$\sigma_0^2 = 10^{-5}$, $\xi = 4.29 \times 10^{-5}$ - Fig. 3(c)], while higher values do not allow reliable syntheses [$\sigma_0^2 = 1$, $\xi = 0.1$ - Fig. 3(c)].

Finally, the plots in Figure 2(d) are concerned with the sensitivity of the *BCS* on N . By analyzing the behaviour of P_{BCS} , it comes out that great care must be exercised on the choice of N to obtain a sparse array matching with a good accuracy the reference one. A good receipt coming also from other heuristic analyses suggests to choose $N \in [5 \times \frac{L}{\lambda}; 100 \times \frac{L}{\lambda}]$.

3.2 *BCS* Assessment - Synthesis of Broadside Patterns

The second set of experiments is aimed at assessing in a more exhaustive fashion the performances of the *BCS* when dealing with broadside patterns. More specifically, Dolph-Chebyshev reference patterns with $L \in \{9.5\lambda, 14.5\lambda, 19.5\lambda\}$ and $PSL \in \{-20, -30, -40\}$ [dB] have been used and the Pareto fronts of the *BCS* solutions are shown in Fig. 4(a). As expected, wider apertures require more elements to reach the accuracy threshold $\xi = 10^{-4}$ (e.g., $P_{BCS}|_{\frac{L}{\lambda}=9.5} = 14$, $P_{BCS}|_{\frac{L}{\lambda}=14.5} = 20$, and $P_{BCS}|_{\frac{L}{\lambda}=19.5} = 36$). On the contrary, P_{BCS} does not generally change when varying the peak sidelobe level (e.g., $P_{BCS}|_{PSL=-20dB} = P_{BCS}|_{PSL=-30dB} = P_{BCS}|_{PSL=-40dB} = 26$). The *BCS* method allows a saving of about 30 – 35% of the array elements with respect to the corresponding uniformly $\frac{\lambda}{2}$ -spaced array still keeping a very accurate pattern matching (i.e., $\xi < 10^{-4}$) [Tab. I]. This implies an increasing of the average

inter-element distance ($\frac{\Delta L}{\lambda/2} \in [1.46, 1.56]$) and, usually, of the minimum spacing between adjacent elements ($\frac{\Delta L_{\min}}{\lambda/2} \in [1.25, 1.56]$) except for the case with $L = 19.5\lambda$ and $PSL = -30$ [dB]. On the other hand, the array aperture only slightly reduces (e.g., $\frac{L_{BCS}}{L_{UNI}} = 0.995$ when $L = 19.5\lambda$ and $PSL = -30$ [dB]) since it controls the mainlobe pattern matching.

As far as the “shape” of the *BCS* Pareto front is concerned [Fig. 4(a)], the plot of the matching error shows a step-like behaviour whatever the array aperture and *PSL* conditions. Moreover, it exists a threshold value of P_{BCS} below which the *BCS* cannot provide an accurate matching for a given $E_{REF}(u)$. For example, the case $L = 19.5\lambda$ - $PSL = -30$ [dB] shows that ξ decreases of more than two orders in magnitude passing from $P_{BCS} = 24$ to $P_{BCS} = 26$. This is visually pointed out in Fig. 4(c) where the plots of $|E_{BCS}(u)|^2$ for $P_{BCS} = \{24, 26\}$ are compared to the reference pattern.

Such a behaviour is further confirmed by the results in Fig. 4(b) where Taylor patterns [1] with transition index $T = 6$ and different sizes (i.e., $L \in \{9.5\lambda, 14.5\lambda, 19.5\lambda\}$) and *PSLs* (i.e., $PSL \in \{-20, -30, -40\}$ [dB]) are taken into account. Also in this case, a small variation of P_{BCS} ($P_{BCS} = 24 \rightarrow 26$) leads to a significant improvement of the reconstruction accuracy ($\xi|_{P_{BCS}=24} = 8.11 \times 10^{-3} \rightarrow \xi|_{P_{BCS}=26} = 3.13 \times 10^{-5}$). The reliable solutions with $\xi < 10^{-4}$ provide also for Taylor syntheses an accurate matching of the reference pattern with negligible errors confined to very low sidelobes, far from the mainlobe [see the inset of Fig. 4(d)], which do not contain relevant portions of the radiated power.

As for the element saving with respect to the $\frac{\lambda}{2}$ -spaced arrangement, the values in Tab. I confirm that $\frac{P_{BCS}}{P_{UNI}} \in [0.65, 0.70]$ as well as the conclusion drawn for the Dolph-Chebyshev patterns on the distribution of the array elements (i.e., $1.43 \leq \frac{\Delta L}{\lambda/2} \leq 1.55$). Concerning the computational issues, the *BCS* turns out to be very efficient ($t_{BCS} < 0.35$ [s] - Tab. I) whatever the broadside reference pattern, despite the non-optimized implementation of the Matlab code.

In order to complete the analysis of the performance of the *BCS* approach when dealing with broadside patterns, comparisons with state-of-the-art techniques have been carried out, as well. Towards this purpose, the *MPM* approach [7]⁽⁶⁾ has been considered because of its efficiency and the enhanced matching accuracy compared to similar methods such as the Prony technique

⁽⁶⁾A MATLAB implementation of the *MPM* has been used for the numerical tests (mpencil function - <http://www.mathworks.se/matlabcentral/index.html>) by setting the default parameters as suggested in [7].

[7]. The results from the analysis of different Dolph-Chebyshev references are summarized in Fig. 5 where the plots of ξ versus P for both *BCS* and *MPM*⁽⁷⁾ arrays are shown. Let us consider the test case characterized by a reference pattern with $PSL = -30$ [dB] defined over a linear aperture of length $L = 9.5\lambda$ [Fig. 5(a)]. In such a case, the *MPM* provides a more accurate fitting than the *BCS* whatever the number of array elements (e.g., $P = 12$: $\xi]_{BCS} = 7.02 \times 10^{-3}$ vs. $\xi]_{MPM} = 1.04 \times 10^{-4}$ [7]) and the *BCS* generally requires a larger P to satisfy the condition $\xi \leq 10^{-4}$ ($P_{BCS} = 14 \rightarrow \xi]_{BCS} = 2.62 \times 10^{-5}$ vs. $P_{MPM} = 13 \rightarrow \xi]_{BCS} = 2.76 \times 10^{-6}$). The *BCS* performances come closer to those of the *MPM* as L increases [$L = 14.5\lambda$ - Fig. 5(b) and $L = 19.5\lambda$ - Fig. 5(c)] and sometimes the *BCS* outperforms the *MPM* in terms of fitting index for both small and large values of P [Figs. 5(b)-5(c)]. Moreover and with reference to Figs. 5(c)-5(e), it results that the efficiency of the *BCS* enhances when PSL reduces. As a matter of fact, the *MPM* overcomes the *BCS* when $L = 19.5\lambda$ and $PSL = -20$ [dB] [Fig. 5(d)], while $\xi_{BCS} < \xi_{MPM}$ for the aperture $L = 19.5\lambda$ with $PSL = -40$ [dB] [Fig. 5(e)] as also pictorially pointed out by the plots of $E_{MPM}(u)$ and $E_{BCS}(u)$ synthesized with the corresponding $P = 26$ -element arrangement [inset of Fig. 5(e)]. As it can be observed, the *BCS* properly matches the reference pattern within the entire visible range, while the *MPM* accuracy worsen near the mainlobe and in the far sidelobes.

Similar conclusions hold true when dealing with Taylor reference patterns. The behavior of ξ versus P (Fig. 6) still indicates that the *MPM* outperforms the *BCS* concerning the minimum P to reach the matching threshold $\xi = 10^{-4}$ when dealing with small arrays and high $PSLs$ [$P_{MPM} = 12 \rightarrow \xi_{MPM} = 9.89 \times 10^{-5}$ vs. $P_{BCS} = 14 \rightarrow \xi_{BCS} = 7.82 \times 10^{-5}$ - Fig. 6(a)], while the *BCS* betters the *MPM* performance for larger L with low peak sidelobe levels [$P_{MPM} = 26 \rightarrow \xi_{MPM} = 2.38 \times 10^{-4}$ vs. $P_{BCS} = 26 \rightarrow \xi_{BCS} = 3.62 \times 10^{-5}$ - Fig. 6(e)]. This is further confirmed by the patterns of the optimal trade-off solutions displayed in the insets of the pictures of Fig. 6.

⁽⁷⁾Please notice that only the *MPM* arrays with *SVD*-truncation parameter below 10^{-3} have been reported in order to guarantee an accurate pattern matching [7].

3.3 BCS Assessment - Synthesis of Shaped Patterns

In order to evaluate the flexibility of the proposed approach, numerical tests concerned with shaped patterns have been also performed. The first experiment deals with the reconstruction of flat top patterns defined over an aperture of $L = 4.5\lambda$ with different PSL s as in [36]. The plots of ξ as a function of P show that neither the MPM nor the BCS is able to reduce the number of array elements of the uniform array (being 0.6λ its inter-element distance) synthesized in [36] still keeping a good accuracy, although the BCS [$P_{BCS} = 10 \rightarrow \xi_{BCS} = 4.55 \times 10^{-6}$ - Fig. 7(a)] reduces the array aperture with respect to [36] ($\frac{L_{BCS}}{L} < 0.97$ - Tab. II). On the contrary, the MPM defines wider arrangements ($\frac{L_{MPM}}{L} = 1.74$), as shown in Fig. 7(d), without yielding a good matching with the reference patterns ($\xi_{MPM} > 2.5 \times 10^{-3}$ - Tab. II). The enhanced accuracy of the BCS is also pointed out by the plots of $E_{REF}(u)$, $E_{BCS}(u)$, and $E_{MPM}(u)$ in the insets of Figs. 7(a)-7(c) related to the arrays with $P_{BCS} = P_{MPM} = 10$. For completeness, the distributions of the array excitations along the array extension are given in Fig. 7(d). As it can be observed and also predicted in [7], the worsening of the performances of the MPM is mainly due to the errors in estimating the element positions caused by the non-negligible values of the imaginary parts of the non-zero roots of the associated eigenvalue problem.

The second experiment considers as reference the *Woodward* pattern with $L = 8.5\lambda$ analyzed in [37]. The plots of ξ versus P show that the BCS faithfully reconstructs the reference pattern synthesizing an array of $P_{BCS} = 12$ elements [$\xi_{BCS} = 2.79 \times 10^{-5}$ - Fig. 8(a)] with a reduction of about $\frac{1}{3}$ of the array elements with respect to the uniform layout ($P_{UNI} = 18$). As a side effect of the approximation, the optimal BCS trade-off slightly improves the PSL of the reference pattern ($P_{BCS} = 12 \rightarrow PSL_{BCS} = -20.2$ [dB] vs. $PSL_{UNI} = -20$ [dB] - Tab. III), as well. On the contrary, both the MPM synthesis in [37] and the MPM pattern generated with $P_{MPM} = 12$ elements do not provide an accurate fitting [$P_{MPM} = 12 \rightarrow \xi_{MPM} = 4.02 \times 10^{-3}$ - Fig. 8(a)], unless using more antenna elements (e.g., $P_{MPM} = 14$), and significantly worsen the PSL ($P_{MPM} = 12 \rightarrow PSL_{MPM} = -13.2$ [dB]) as highlighted by the plots of the associated patterns [Fig. 8(b)]. For completeness, the behaviour of the array excitations and the corresponding figures of merit are reported in Fig. 8(c) and Tab. III, respectively. As for the computational costs, the BCS still retains the numerical efficiency proved in synthesizing

broadside patterns (Tab. III).

Similar conclusions can be also drawn when considering wider reference apertures. For example, with reference to a Woodward reference pattern with $L = 19.5\lambda$ [Fig. 9(a)], the *BCS* yields an accurate approximation with less elements than the *MPM* ($P_{BCS} = 26$ vs. $P_{MPM} = 28$). Moreover, the accuracy of the *MPM* significantly worsens when using the same number of active elements of the *BCS* solution [$P = 26 - \xi_{MPM} = 4.81 \times 10^{-2}$, $PSL_{MPM} = -3.6$ [dB] vs. $\xi_{BCS} = 3.52 \times 10^{-5}$, $PSL_{BCS} = -17.4$ - Tab. IV and Fig. 9(b)]. As for the array arrangement, the *BCS* provides a more widely-spaced design characterized by the following parameters: $\frac{\Delta L_{\min}}{\lambda/2} = 0.975$ and $\frac{\Delta L}{\lambda/2} = 1.56$ (Tab. IV).

3.4 *BCS* Assessment - Constrained Synthesis

This section is devoted to assess the reliability of the *BCS* approach in solving constrained synthesis problems (i.e., matching a reference pattern under some explicit geometric and/or radiation constraints). Towards this aim, the synthesis of a Dolph-Chebyshev pattern with $L = 19.5\lambda$ and $PSL = -30$ [dB] under different synthesis constraints has been addressed.

The first test case has been formulated by enforcing the pattern matching constraints in the angular region $u_k \notin [u_m, u_M]$, being $u_m = 0.5$ and $u_M = 0.6$. As desired, the pattern of the optimal *BCS* trade-off solution ($\xi = 3.71 \times 10^{-5}$ - Tab. V) fits in a faithful way the reference one within the constrained region as well as in the transition regions close to the unconstrained angular range [Fig. 10(b)]. It is also of interest to observe that the distribution of the array excitations of the *BCS* synthesis and those of the uniform array quite significantly differ [Fig. 10(a)].

To further verify the efficiency of the *BCS* to include pattern constraints in the synthesis process without affecting the reliability of the matching in the remaining portion of the pattern, the constraint has been moved in another region of the visible range by setting $u_m = 0.8$ and $u_M = 1.0$. As expected, the trade-off pattern carefully matches the reference in the constrained region ($\xi = 6.81 \times 10^{-5}$ - Tab. V), while uncontrolled lobes appear for $u > 0.8$ [Fig. 11(b)]. The use of a directive element [e.g., a $\cos(\theta)$ radiating element] might then enable the control of the sidelobes in the whole visible region [Fig. 11(b)] with a significant saving of active elements

in comparison with the uniform array synthesizing the entire Dolph pattern ($P_{BCS} = 21$ vs. $P_{UNI} = 40$).

The last part of the numerical assessment is aimed at analyzing the capability of the *BCS* approach to also take into account geometrical constraints. Towards this end and considering the same reference pattern of the previous experiments, two different aperture-blockage problems have been defined: (i) $d_n \notin [5.3\lambda, 6.5\lambda]$ and (ii) $d_n \notin [0.0\lambda, 1.0\lambda]$. The plots of the synthesized trade-off arrangements assess the effectiveness and reliability of the *BCS* technique in constraining the element positions to desired locations [Fig. 12(a) and 13(a)], while designing sparse arrangements ($\Delta L > \lambda/2$ - Tab. V) with reduced apertures ($L_{BCS} < 19.47$), as well. It is also worthwhile to point out that, notwithstanding the non-negligible reduction of the admissible spatial region for the array elements (more than 10% in both cases), the $E_{BCS}(u)$ pattern matches the reference $E_{REF}(u)$ with a great care [Fig. 12(b) and Fig. 13(b)] as confirmed by the values of the matching index [(i) $\xi = 5.82 \times 10^{-6}$ and (ii) $\xi = 4.81 \times 10^{-5}$ - Tab. V].

4 Conclusions

In this paper, the *BCS* has been applied to the synthesis of sparse arrays with desired radiation properties. The pattern matching problem has been properly reformulated in a suitable Bayesian framework and successively solved with a fast solver. An extensive numerical validation has been carried out dealing with different reference patterns, array sizes, and constraints to assess the feasibility and reliability of the *BCS* approach as well as its efficiency, flexibility, and accuracy. Selected comparisons with state-of-the-art techniques have highlighted the advantages and limitations of the *BCS* synthesis in terms of sensitivity on control parameters, performances, and computational complexity. The proposed technique has shown the following main features:

- several tradeoffs solutions can be easily obtained by means of simple modifications of the control parameters (σ^2 , u_k , d_n , and σ_0^2) (Sect. 3.1);
- *BCS* favorably compares with state-of-the-art techniques such as the *MPM* [7] in terms of accuracy, array sparseness, and computational burden when matching reference broad-side patterns (Sect. 3.2);

- on average the number of active elements in a *BCS* array turns out to be smaller than the corresponding uniform arrangement ($P_{BCS} \approx 0.7 \div 0.65 P_{UNI}$) still providing a high accuracy in matching the reference pattern (i.e., $\xi \leq 10^{-4}$);
- *BCS* usually outperforms *MPM* when dealing with shaped beampatterns (Sect. 3.3);
- application-specific constraints on either the radiation pattern or the geometrical characteristics of the array can be easily and efficiently taken into account (Sect. 3.4).

Subjects of future researches will be the analysis of the mutual coupling effects in the presence of realistic array elements as well as an enhanced exploitation of directive elements. Further extensions, out-of-the-scope of the present paper, will concern with complex excitations and non-symmetric layouts.

Acknowledgements

The authors wish to thank Dr. S. Ji, Dr. Y. Xue, and Prof. L. Carin for sharing the *BCS* code online.

Appendix

- Sequential Solver for the Maximization of $\mathcal{L}(\mathbf{a}, \sigma^2)$

The marginal likelihood maximization algorithm proposed in [34] is hereinafter customized to deal with user-defined pattern matching problems. Starting from the knowledge of \mathbf{E}_{REF} and Ψ , the following sequence is iteratively (r being the iteration index) applied:

1. **Initialization** ($r = 0$) - Set $[\sigma^2]^{(r)} = \text{var}[\mathbf{E}_{REF}] \times \sigma_0^2$ and the n -th entry of the diagonal matrix $A^{(r)} \triangleq \text{diag}(a_1^{(r)}, \dots, a_N^{(r)})$ as follows

$$a_n^{(r)} = \frac{\|\psi_n\|^4}{\|\psi_n^T \mathbf{E}_{REF}\|^2 - [\sigma^2]^{(r)} \|\psi_n\|^2} \quad (17)$$

if $n = \hat{n}$ and $a_n^{(r)} = \infty$ otherwise, \hat{n} and ψ_n being randomly picked integers within $[1, N]$ and the n -th column of Ψ , respectively;

2. **Update** - Evaluate $\Sigma^{(r)} = \Sigma \left(A^{(r)}, [\sigma^2]^{(r)} \right)$ and $\mu^{(r)} = \mu \left(A^{(r)}, [\sigma^2]^{(r)} \right)$ to compute the *sparsity* factors $s_n^{(r)} = \psi_n^T C_{-n}^{-1} \psi_n$, $n = 1, \dots, N$ and the *quality* factors $z_n^{(r)} = \psi_n^T C_{-n}^{-1} \mathbf{E}_{REF}$, $n = 1, \dots, N$ where $C_{-n} = C - a_n^{-1} \psi_n \psi_n^T$;
3. **Candidate Basis Vector Evaluation** - Select the r -th candidate basis vector⁽⁸⁾ ψ_n , $n = r$, and compute $\Theta_n^{(r)} = \left(z_n^{(r)} \right)^2 - s_n^{(r)}$. If $\Theta_n^{(r)} > 0$, then update the value of $a_n^{(r)}$ by means of (17), otherwise set $a_n^{(r)} = \infty$;
4. **Convergence Check** - Compute the value of $\Theta_n^{(r)} \forall n \in 1, \dots, N$. If $\Theta_n^{(r)} \leq \tau \forall n$ (τ being the *tolerance factor* usually set to 10^{-8} [35]), then terminate. Otherwise, update the iteration index ($r \leftarrow r + 1$) and go to step 2.

⁽⁸⁾Please refer to [34] for a review of the strategies for candidate selection.

References

- [1] C. A. Balanis, *Antenna Theory: Analysis and Design*, 2nd ed. New York: Wiley, 1997.
- [2] R. J. Mailloux, *Phased Array Antenna Handbook*, 2nd ed. Norwood, MA: Artech House, 2005.
- [3] R. M. Leahy and B. D. Jeffs, "On the design of maximally sparse beamforming arrays", *IEEE Trans. Antennas Propagat.*, vol. 39, no. 8, pp. 1178-1187, Aug. 1991.
- [4] D. King, R. Packard, and R. Thomas, "Unequally spaced, broad-band antenna arrays," *IRE Trans. Antennas Propagat.*, vol. AP-8, pp. 380-384, Jul. 1960.
- [5] A. Maffett, "Array factors with nonuniform spacing arrays," *IRE Trans. Antennas Propagat.*, vol. AP-10, pp. 131-136, Mar. 1962.
- [6] N. Balakrishnan, P. Murthy, and S. Ramakrishna, "Synthesis of antenna arrays with spatial and excitation constraints," *IEEE Trans. Antennas Propagat.*, vol. AP-29, pp. 690-696, Sep. 1962.
- [7] Y. Liu, Z. Nie, and Q. H. Liu, "Reducing the number of antenna elements in a linear antenna array by the matrix pencil method," *IEEE Trans. Antennas Propagat.*, vol. 56, no. 9, pp. 2955-2962, Sep. 2008.
- [8] R. F. Harrington, "Sidelobe reduction by nonuniform element spacing," *IEEE Trans. Antennas Propagat.*, vol. AP-9, p. 187, Mar. 1961.
- [9] M. G. Andreasan, "Linear arrays with variable interelement spacings," *IEEE Trans. Antennas Propagat.*, vol. AP-10, pp. 137-143, Mar. 1962.
- [10] A. Ishimaru, "Theory of unequally-spaced arrays," *IEEE Trans. Antennas Propagat.*, vol. AP-11, pp. 691-702, Nov. 1962.
- [11] Y. T. Lo, "A mathematical theory of antenna arrays with randomly spaced elements," *IEEE Trans. Antennas Propagat.*, vol. 12, no. 3, pp. 257-268, May 1964.

- [12] M. I. Skolnik, G. Nemhauser, and J. W. Sherman, "Dynamic programming applied to unequally-spaced arrays", *IRE Trans. Antennas Propagat.*, vol. AP-12, pp. 35-43, Jan. 1964.
- [13] J. Perini and M. Idselis, "Note on antenna pattern synthesis using numerical iterative methods," *IEEE Trans. Antennas Propag.*, vol. 19, no. 2, pp. 284-286, Mar. 1971.
- [14] R. W. Redlich, "Iterative least-squares of nonuniformly spaced linear arrays," *IEEE Trans. Antennas Propag.*, vol. AP-21, no. 1, pp. 106-108, Jan. 1973.
- [15] B. Steinberg, "The peak sidelobe of the phased array having randomly located elements," *IEEE Trans. Antennas Propag.*, vol. 20, no. 2, pp. 129-136, Mar. 1972.
- [16] P. Jarske, T. Sramaki, S. K. Mitra, and Y. Neuvo, "On the properties and design of nonuniformly spaced linear arrays," *IEEE Trans. Acoust., Speech, Signal Processing*, vol. 36, pp. 372-380, Mar. 1988.
- [17] R. L. Haupt, "Thinned arrays using genetic algorithms," *IEEE Trans. Antennas Propag.*, vol. 42, no. 7, pp. 993-999, Jul. 1994.
- [18] V. Murino, A. Trucco, and C. S. Regazzoni, "Synthesis of unequally spaced arrays by simulated annealing," *IEEE Trans. Signal Processing*, vol. 44, no. 1, pp. 119-123, Jan. 1996.
- [19] S. Holm, B. Elgetun, and G. Dahl, "Properties of the beam pattern of weight- and layout-optimized sparse arrays," *IEEE Trans. Ultrason., Ferroelectr., Freq. Control*, vol. 44, no. 5, pp. 983-991, Sep. 1997.
- [20] A. Trucco and V. Murino, "Stochastic optimization of linear sparse arrays," *IEEE J. Oceanic Engineering*, vol. 24, no. 3, pp. 291-299, Jul. 1999.
- [21] B. P. Kumar and G. R. Branner, "Design of unequally spaced arrays for performance improvement," *IEEE Trans. Antennas Propag.*, vol. 47, pp. 511-523, Mar. 1999.
- [22] D. G. Leeper, "Isophoric arrays - massively thinned phased arrays with well-controlled sidelobes," *IEEE Trans. Antennas Propag.*, vol. 47, no. 12, pp. 1825-1835, Dec. 1999.

- [23] F. B. T. Marchaud, G. D. de Villiers, and E. R. Pike, "Element positioning for linear arrays using generalized Gaussian quadrature," *IEEE Trans. Antennas Propag.*, vol. 51, no. 6, pp. 1357-1363, Jun. 2003.
- [24] D. G. Kurup, M. Himdi, and A. Rydberg, "Synthesis of uniform amplitude unequally spaced antenna array using the differential evolution algorithm," *IEEE Trans. Antennas Propag.*, vol. 51, pp. 2210-2217, Sep. 2003.
- [25] S. Caorsi, A. Lommi, A. Massa, and M. Pastorino, "Peak sidelobe reduction with a hybrid approach based on GAs and difference sets," *IEEE Trans. Antennas Propag.*, vol. 52, no. 4, pp. 1116-1121, Apr. 2004.
- [26] B. P. Kumar and G. R. Branner, "Generalized analytical technique for the synthesis of unequally spaced arrays with linear, planar, cylindrical or spherical geometry," *IEEE Trans. Antennas Propag.*, vol. 53, pp. 621-633, Feb. 2005.
- [27] T. G. Spence and D. H. Werner, "Thinning of aperiodic antenna arrays for low side-lobe levels and broadband operation using genetic algorithms," Proc. IEEE Antennas and Propagation Society International Symposium 2006, pp. 2059-2062, 9-14 Jul. 2006.
- [28] R. L. Haupt and D. H. Werner, *Genetic algorithms in electromagnetics*. Hoboken, NJ: Wiley, 2007.
- [29] P. J. Bevelacqua and C. A. Balanis, "Minimum sidelobe levels for linear arrays," *IEEE Trans. Antennas Propag.*, vol. 55, pp. 2210-2217, Dec. 2007.
- [30] G. Oliveri, M. Donelli, and A. Massa, "Linear array thinning exploiting almost difference sets," *IEEE Trans. Antennas Propag.*, vol. 57, no. 12, pp. 3800-3812, Dec. 2009.
- [31] S. Ji, Y. Xue, and L. Carin, "Bayesian compressive sensing," *IEEE Trans. Signal Process.*, vol. 56, no. 6, pp. 2346-2356, Jun. 2008.
- [32] M. E. Tipping, "Sparse bayesian learning and the relevance vector machine", *J. Machine Learning Res.*, vol 1, pp. 211-244, 2001.

- [33] A. C. Faul and M. E. Tipping, "Analysis of sparse Bayesian learning," in Advances in Neural Information Processing Systems (NIPS 14), T. G. Dietterich, S. Becker, and Z. Ghahramani, Eds., 2002, pp. 383-389 [Online]. Available: <http://citeseer.ist.psu.edu/faul01analysis.html>
- [34] M. E. Tipping and A. C. Faul, "Fast marginal likelihood maximization for sparse Bayesian models," in Proc. 9th Int. Workshop Artificial Intelligence and Statistics, C.M. Bishop and B. J. Frey, Eds., 2003 [Online]. Available: <http://citeseer.ist.psu.edu/611465.html>
- [35] S. Ji, Y. Xue, and L. Carin, "Bayesian compressive sensing code", 2009 [Online]. Available: <http://people.ee.duke.edu/~lihan/cs/>
- [36] F. Ares and E. Moreno, "The convolution applied on the synthesis shaped beam," in *Proceedings of the 20th European Microwave Conference*, vol. 2, pp. 1491-1494, Oct. 1990.
- [37] S. Yang, Y. Liu, Q. H. Liu, "Combined strategies based on matrix pencil method and tabu search algorithm to minimize elements of non-uniform antenna array", *Progress in Electromagnetic Research B*, vol. 18, pp. 259-277, 2009.

FIGURE CAPTIONS

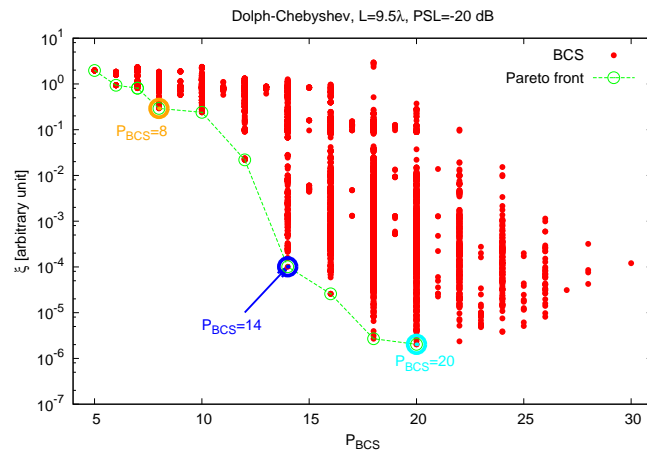
- **Figure 1.** *BCS Sensitivity Analysis (Dolph-Chebyshev: $L = 9.5\lambda$, $PSL = -20$ dB)* - Plot of the representative points of a set of *BCS* solutions in the (ξ, P_{BCS}) plane (a). Power patterns (b) and corresponding layouts (c) of the reference and of a set of representative *BCS* arrays.
- **Figure 2.** *BCS Sensitivity Analysis (Dolph-Chebyshev: $L = 9.5\lambda$, $PSL = -20$ dB)* - Behaviours of ξ and P_{BCS} versus (a) K , (b) σ^2 , (c) σ_0^2 , and (d) N .
- **Figure 3.** *BCS Sensitivity Analysis (Dolph-Chebyshev: $L = 9.5\lambda$, $PSL = -20$ dB)* - Plots of $|E_{REF}(u) - E_{BCS}(u)|^2$ of representative *BCS* solutions computed at different values of (a) K , (b) σ^2 , (c) σ_0^2 , and (d) N .
- **Figure 4.** *BCS Assessment (Broadside Pattern Synthesis)* - Pareto fronts in the (ξ, P_{BCS}) plane (a)(b) and power patterns (c)(d) of representative *BCS* solutions when matching (a)(c) Dolph-Chebyshev and (b)(d) Taylor reference patterns.
- **Figure 5.** *BCS Assessment (Broadside Pattern Synthesis)* - Representative points in the (ξ, P) plane of *BCS* and *MPM* solutions synthesized when matching the reference *Dolph-Chebyshev* patterns characterized by: (a) $L = 9.5\lambda$ - $PSL = -30$ [dB], (b) $L = 14.5\lambda$ - $PSL = -30$ [dB], (c) $L = 19.5\lambda$ - $PSL = -30$ [dB], (d) $L = 19.5\lambda$ - $PSL = -20$ [dB], and (e) $L = 19.5\lambda$ - $PSL = -40$ [dB].
- **Figure 6.** *BCS Assessment (Broadside Pattern Synthesis)* - Representative points in the (ξ, P) plane of *BCS* and *MPM* solutions synthesized when matching the reference *Taylor* patterns characterized by: (a) $L = 9.5\lambda$ - $PSL = -30$ [dB], (b) $L = 14.5\lambda$ - $PSL = -30$ [dB], (c) $L = 19.5\lambda$ - $PSL = -30$ [dB], (d) $L = 19.5\lambda$ - $PSL = -20$ [dB], and (e) $L = 19.5\lambda$, $PSL = -40$ [dB].
- **Figure 7.** *BCS Assessment (Shaped Pattern Synthesis: $L = 5.4\lambda$ [36])* - Representative points in the (ξ, P) plane of *BCS* and *MPM* solutions synthesized when matching the reference *Shaped* patterns [36] characterized by: (a) $PSL = -20$ dB, (b) $PSL = -30$ [dB], and (c) $PSL = -40$ [dB]. Array excitations (d).

- **Figure 8.** *BCS Assessment (Flat-Top Pattern Synthesis: $L = 8.5\lambda$ [37])* - Representative points in the (ξ, P) plane of *BCS* and *MPM* solutions (a), optimal trade-off beam patterns (b), and associated array excitations (c).
- **Figure 9.** *BCS Assessment (Flat Top Pattern Synthesis: $L = 19.5\lambda$)* - Representative points in the (ξ, P) plane of *BCS* and *MPM* solutions (a), optimal trade-off beam patterns (b), and associated array excitations (c).
- **Figure 10.** *BCS Assessment [Constrained Synthesis - Dolph-Chebyshev: $L = 19.5\lambda$, $u_k \notin (0.45, 0.55)$]* - Array excitations (a) and power patterns (b).
- **Figure 11.** *BCS Assessment (Constrained Synthesis - Dolph-Chebyshev: $L = 19.5\lambda$, $u_k \notin (0.8, 1.0)$)* - Array excitations (a) and power patterns when using isotropic or directive elements (b).
- **Figure 12.** *BCS Assessment [Constrained Synthesis - Dolph-Chebyshev: $L = 19.5\lambda$, $d_n \notin (5.3\lambda, 6.5\lambda)$]* - Array excitations (a) and power patterns (b).
- **Figure 13.** *BCS Assessment [Constrained Synthesis - Dolph-Chebyshev: $L = 19.5\lambda$, $d_n \notin (0.0\lambda, 1.0\lambda)$]* - Array excitations (a) and power patterns (b).

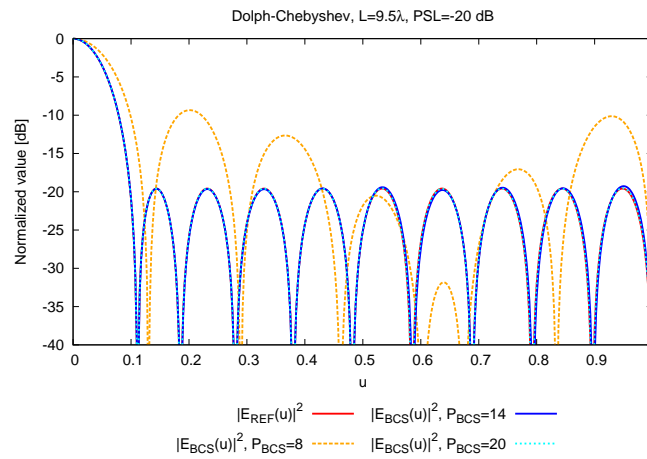
TABLE CAPTIONS

- **Table I.** *BCS Assessment (Broadside Pattern Synthesis)* - Array performance indexes.
- **Table II.** *BCS Assessment (Shaped Pattern Synthesis: $L = 5.4\lambda$ [36])* - Array performance indexes.
- **Table III.** *BCS Assessment (Shaped Pattern Synthesis: $L = 8.5\lambda$ [37])* - Array performance indexes.
- **Table IV.** *BCS Assessment (Shaped Pattern Synthesis: $L = 19.5\lambda$)* - Array performance indexes.

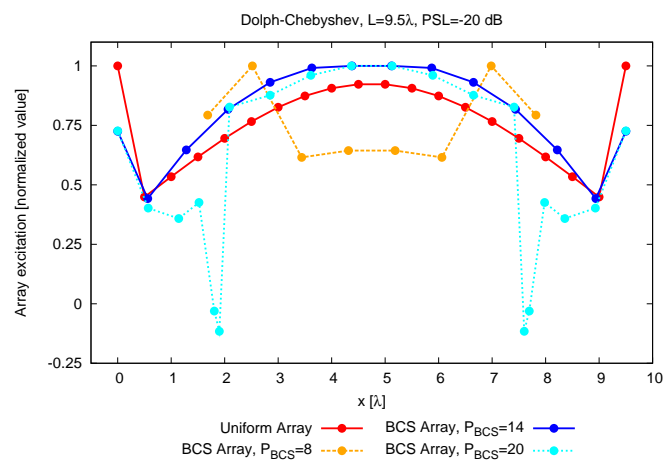
- **Table V.** *BCS Assessment (Constrained Synthesis - Dolph-Chebyshev: $L = 19.5\lambda$)* - Array performance indexes.



(a)



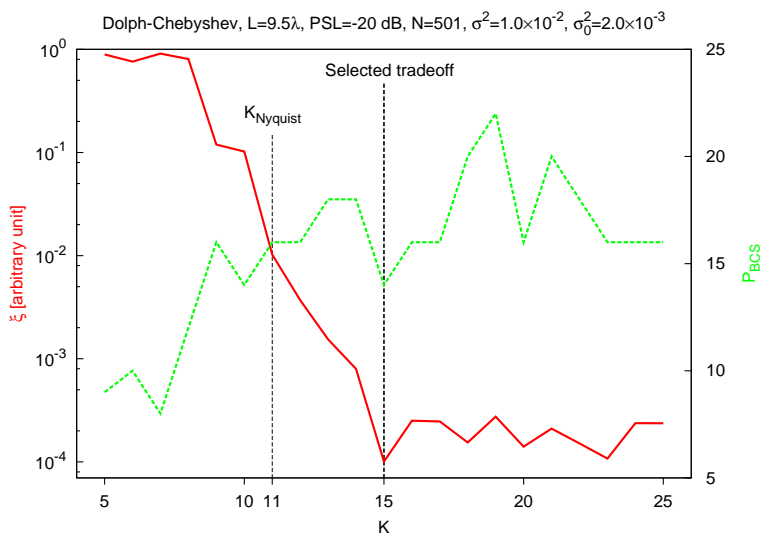
(b)



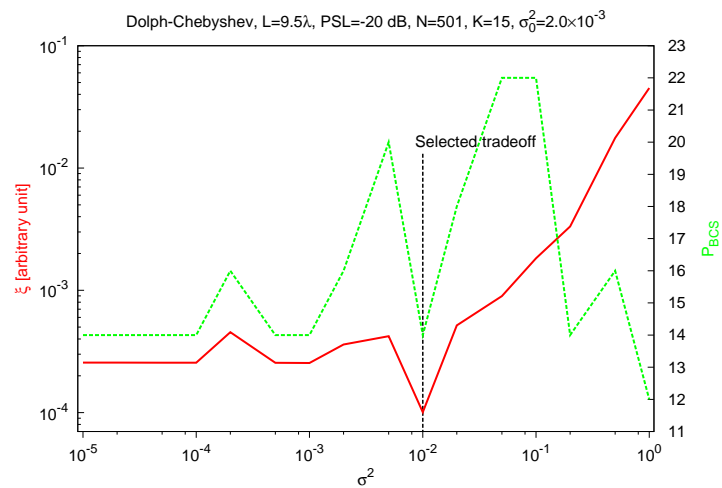
(c)

Figure 1 - G. Oliveri et al., “Bayesian Compressive Sampling for...”

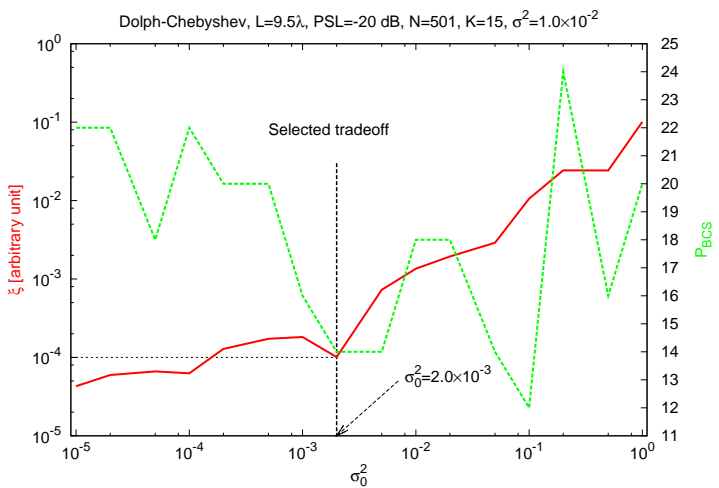
Figure 2 - G. Oliveri et al., "Bayesian Compressive Sampling for..."



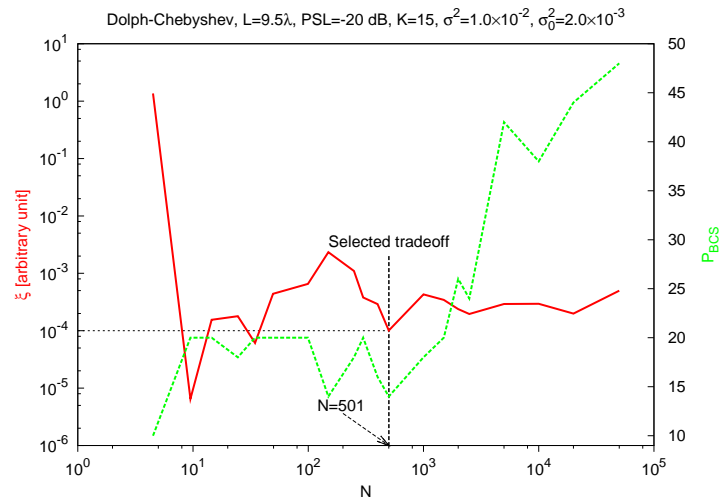
(a)



(b)

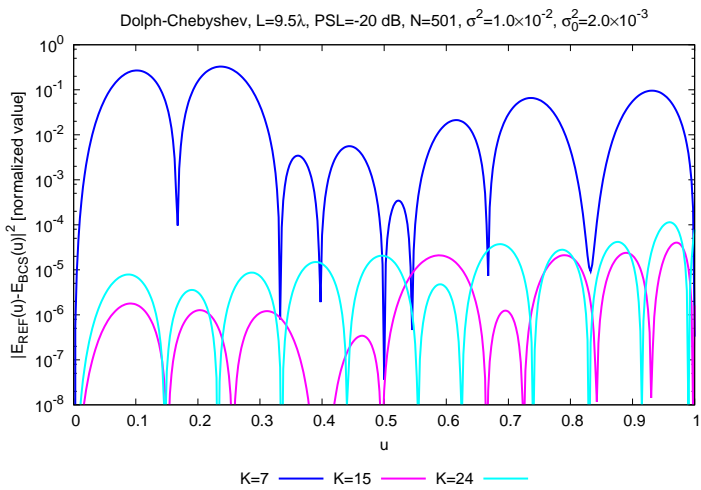


(c)

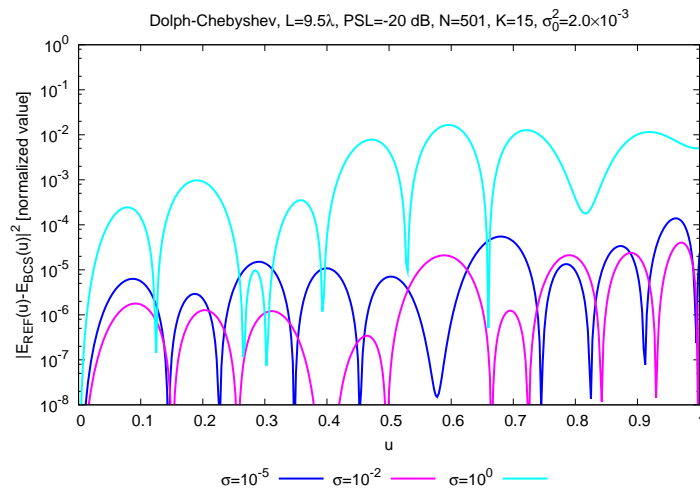


(d)

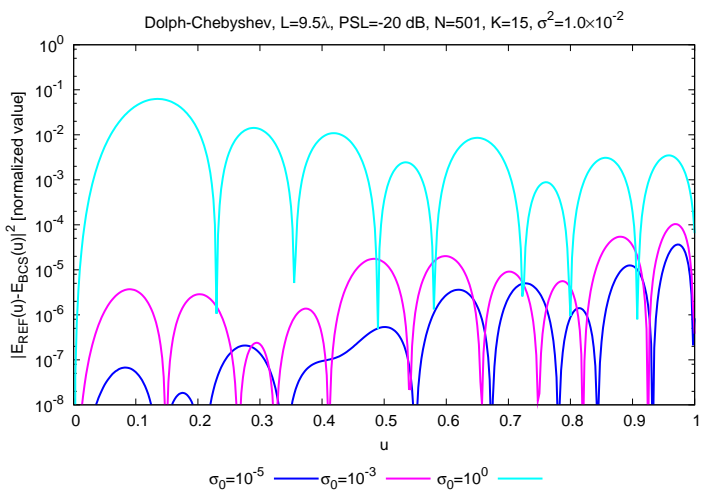
Figure 3 - G. Oliveri et al., "Bayesian Compressive Sampling for..."



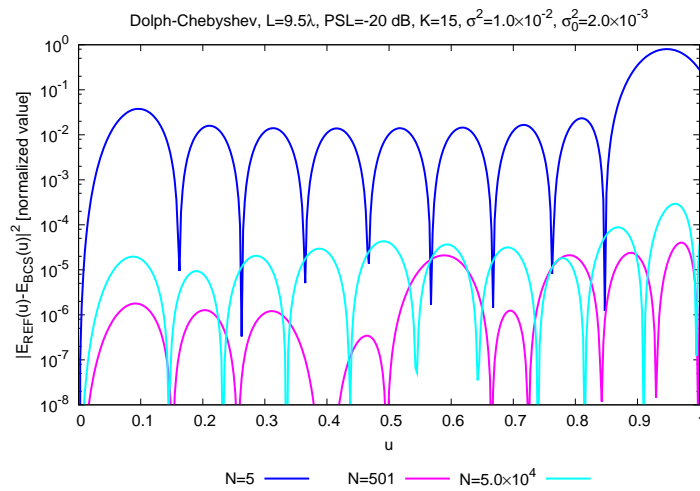
(a)



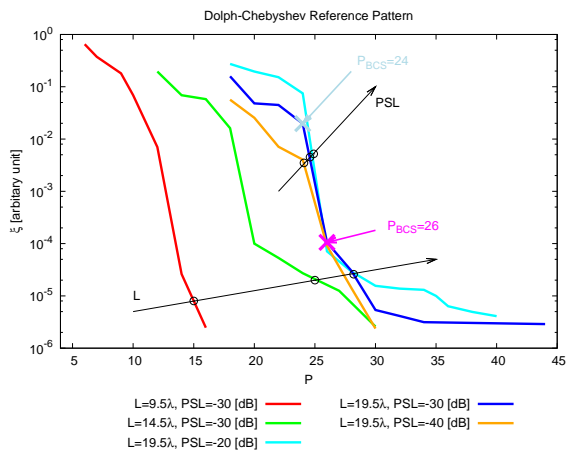
(b)



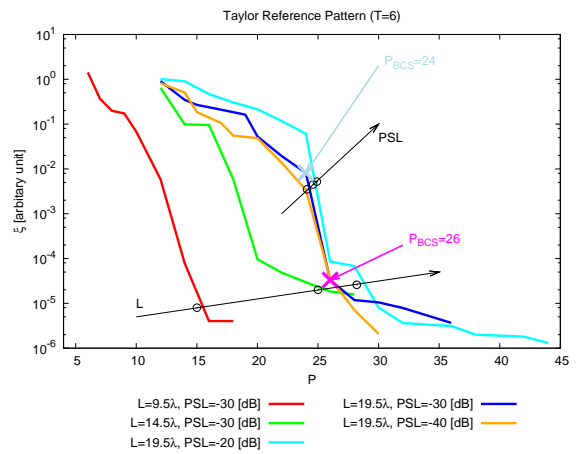
(c)



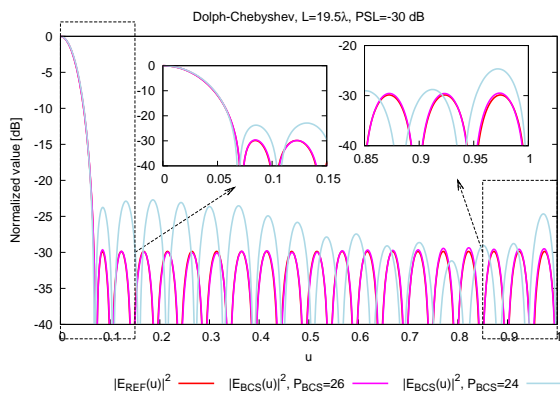
(d)



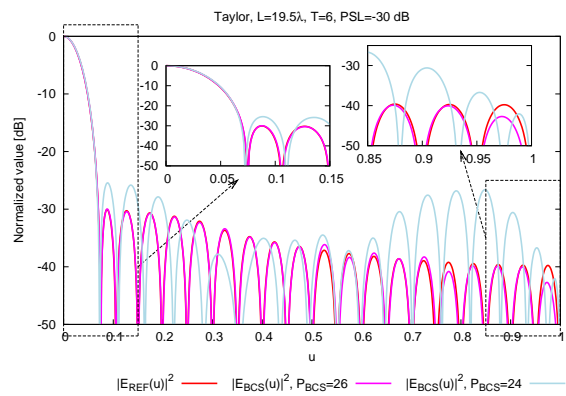
(a)



(b)

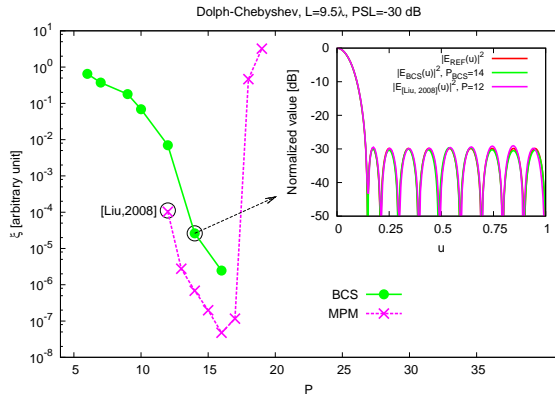


(c)

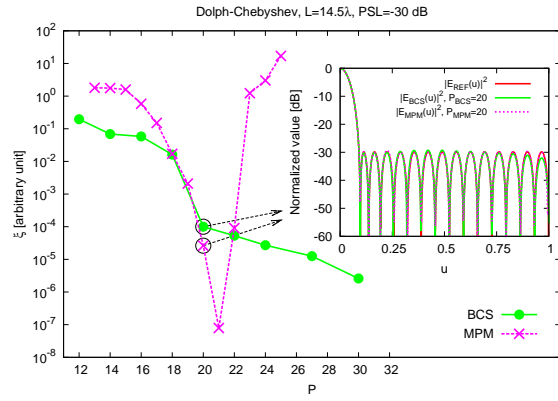


(d)

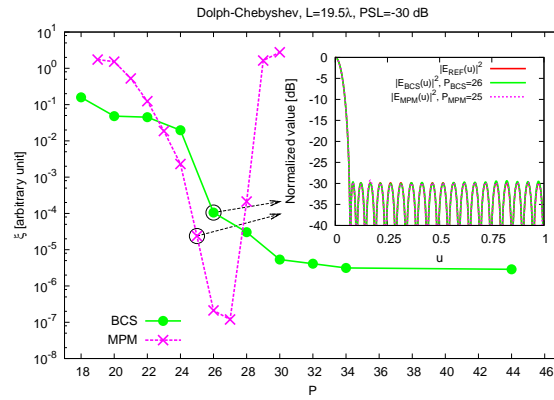
Figure 4 - G. Oliveri et al., "Bayesian Compressive Sampling for..."



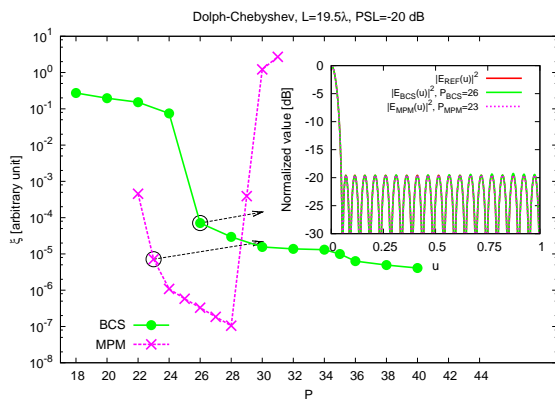
(a)



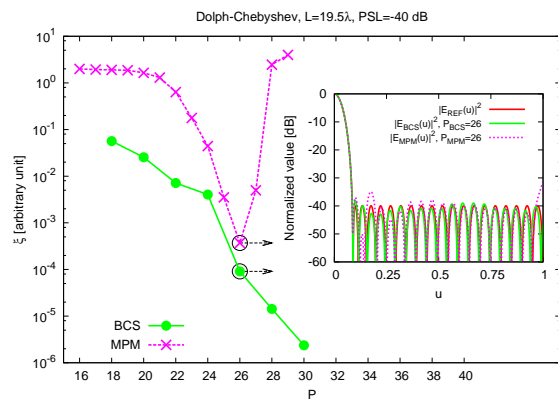
(b)



(c)

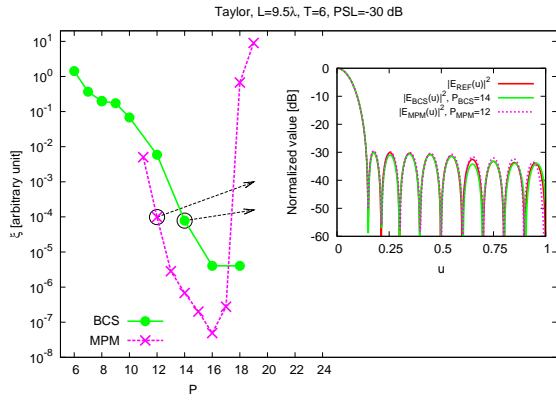


(d)

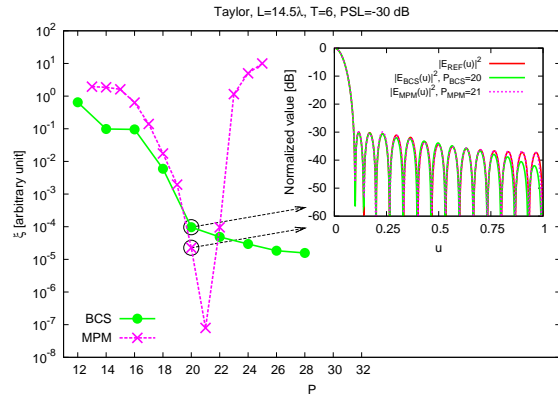


(e)

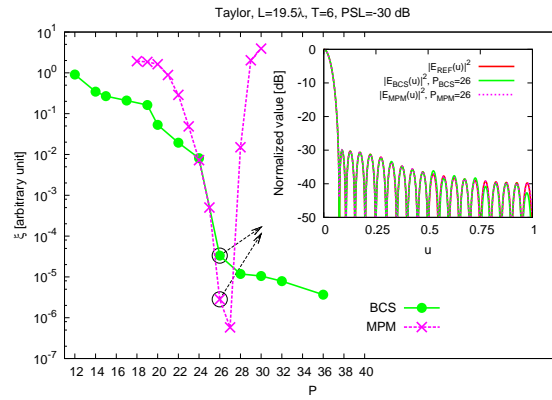
Figure 5 - G. Oliveri et al., "Bayesian Compressive Sampling for..."



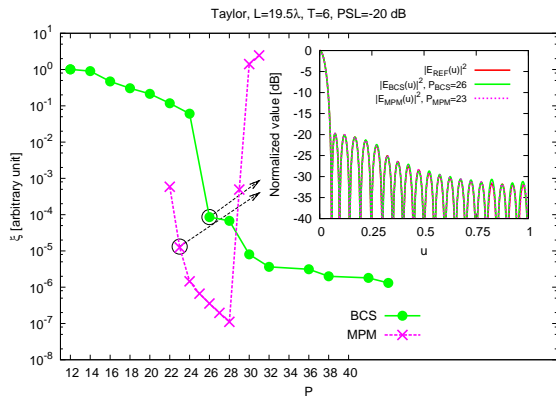
(a)



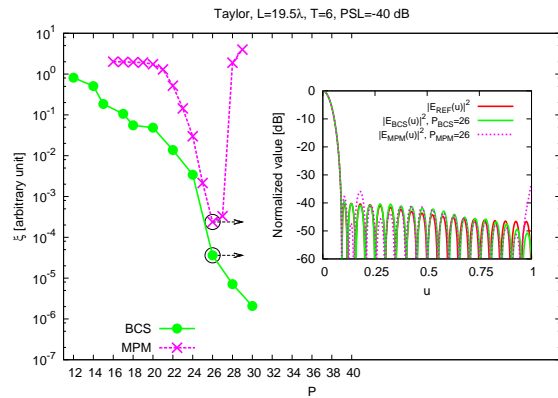
(b)



(c)



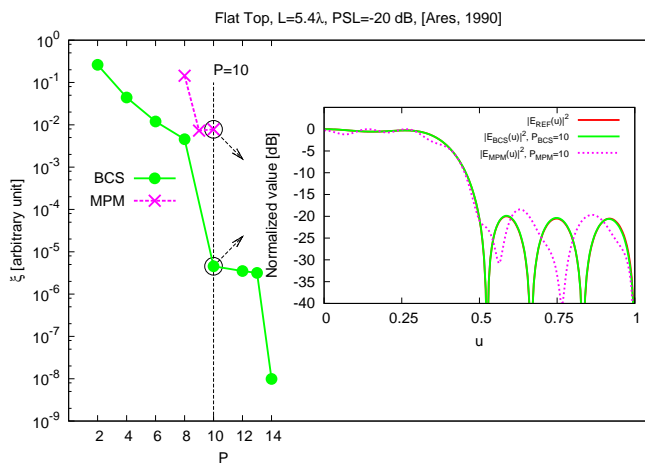
(d)



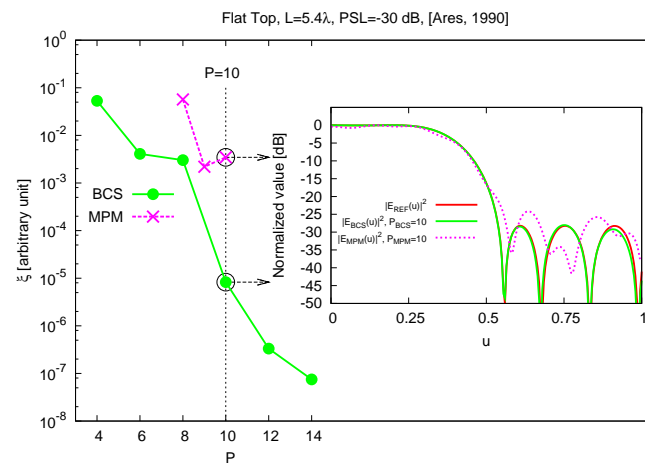
(e)

Figure 6 - G. Oliveri et al., "Bayesian Compressive Sampling for..."

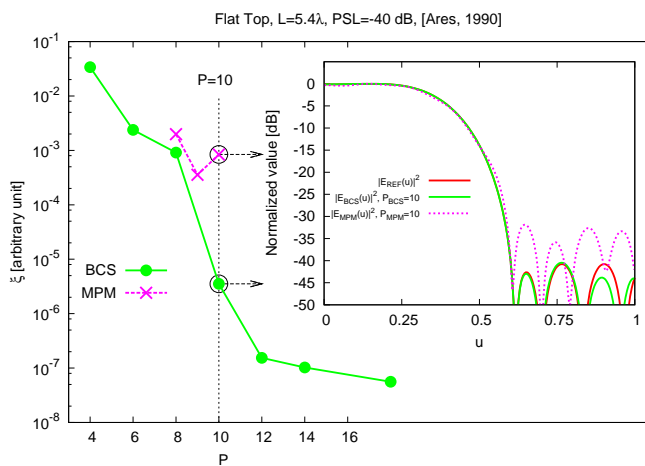
Figure 7 - G. Oliveri et al., "Bayesian Compressive Sampling for..."



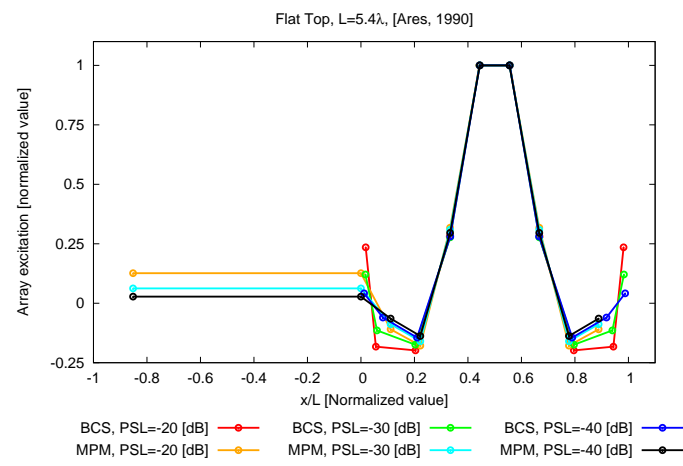
(a)



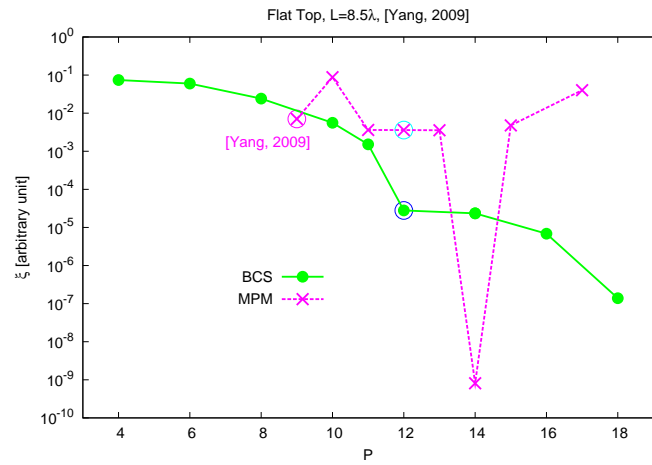
(b)



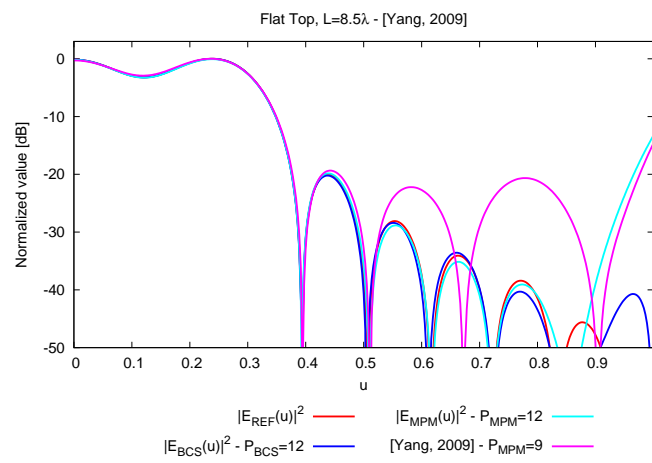
(c)



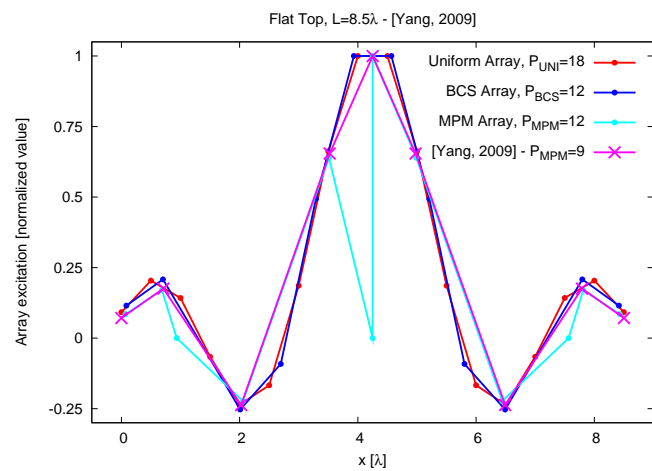
(d)



(a)

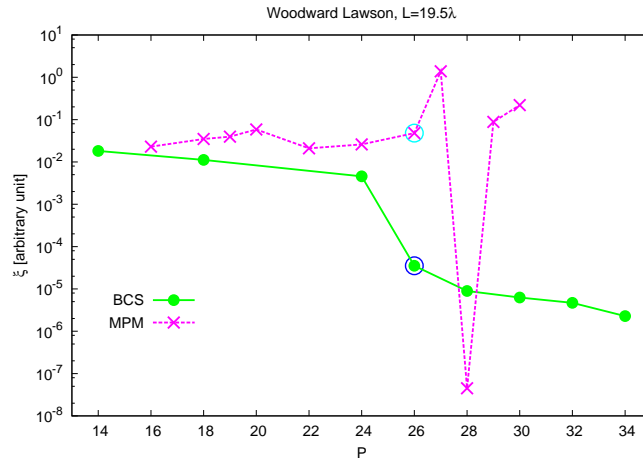


(b)

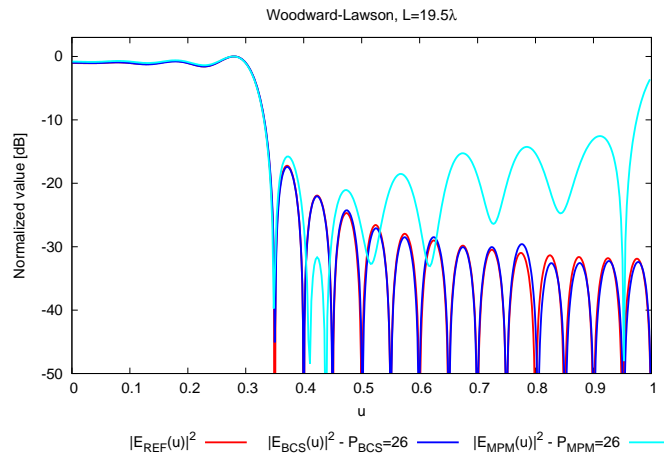


(c)

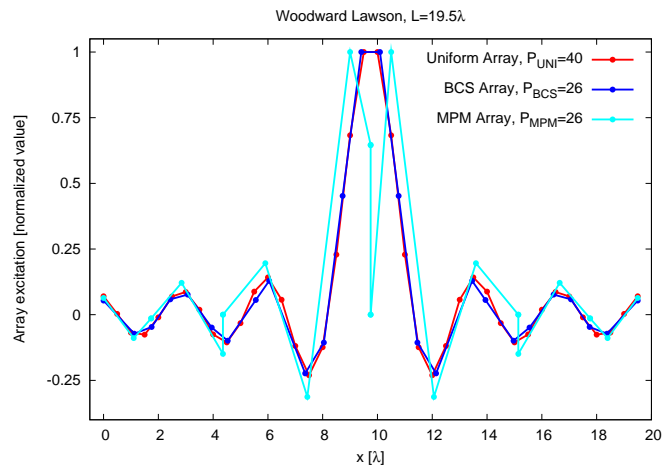
Figure 8 - G. Oliveri et al., "Bayesian Compressive Sampling for..."



(a)

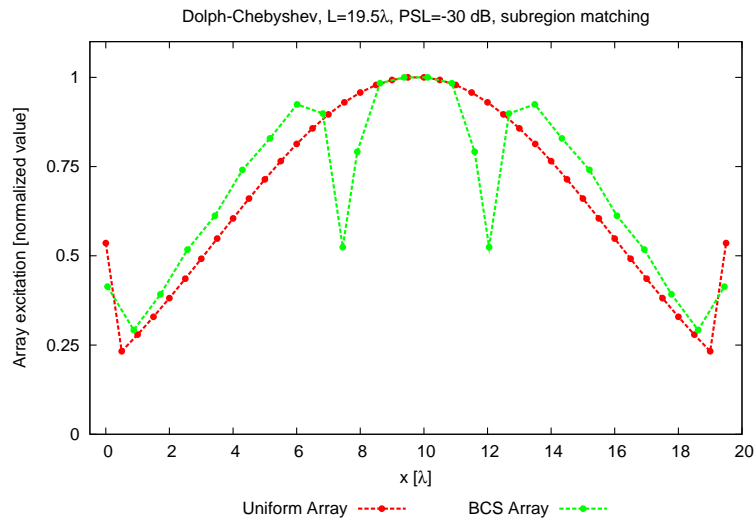


(b)

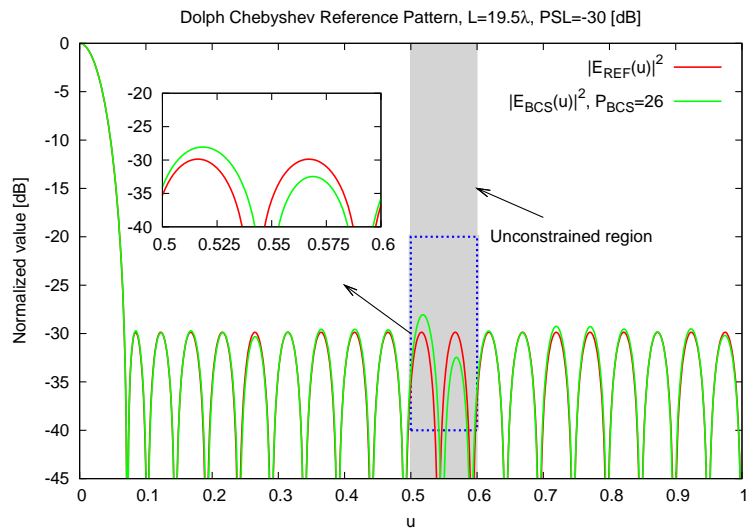


(c)

Figure 9 - G. Oliveri et al., “Bayesian Compressive Sampling for...”

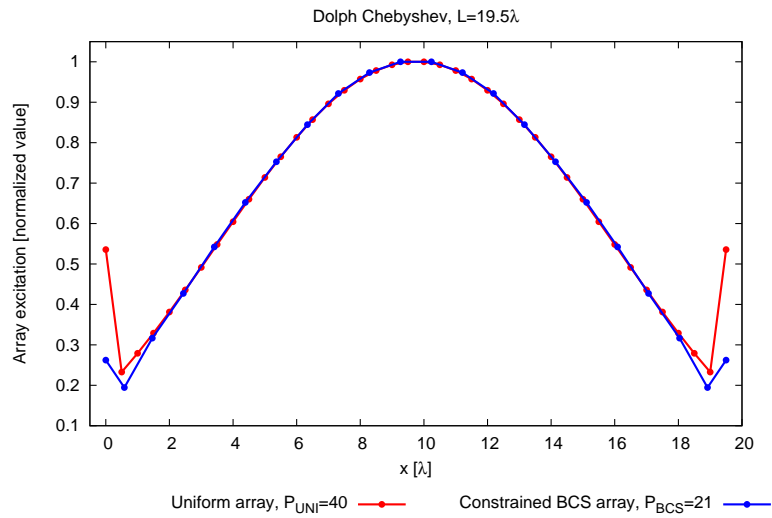


(a)

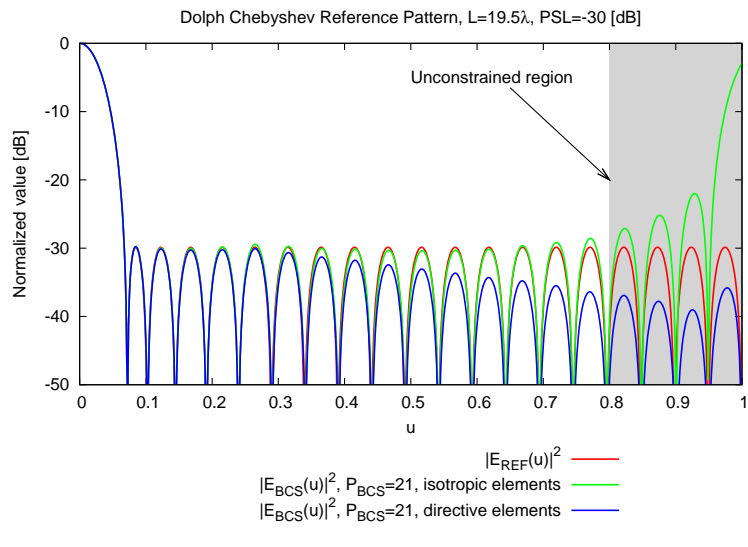


(b)

Figure 10 - G. Oliveri et al., “Bayesian Compressive Sampling for...”

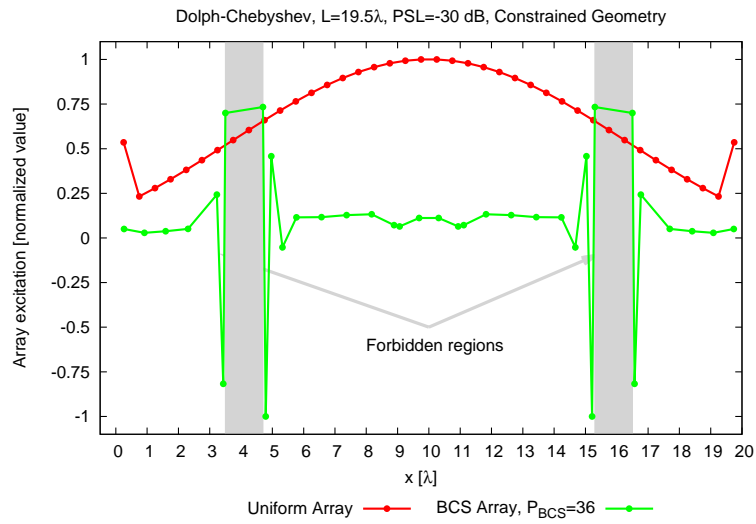


(a)

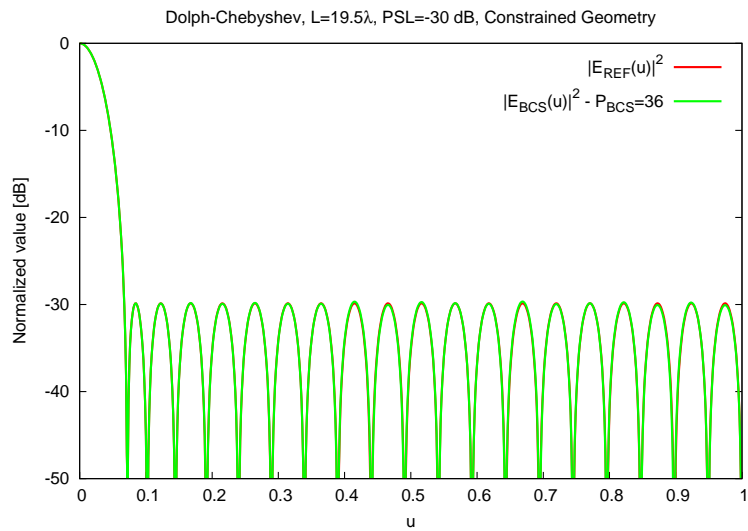


(b)

Figure 11 - G. Oliveri et al., “Bayesian Compressive Sampling for...”

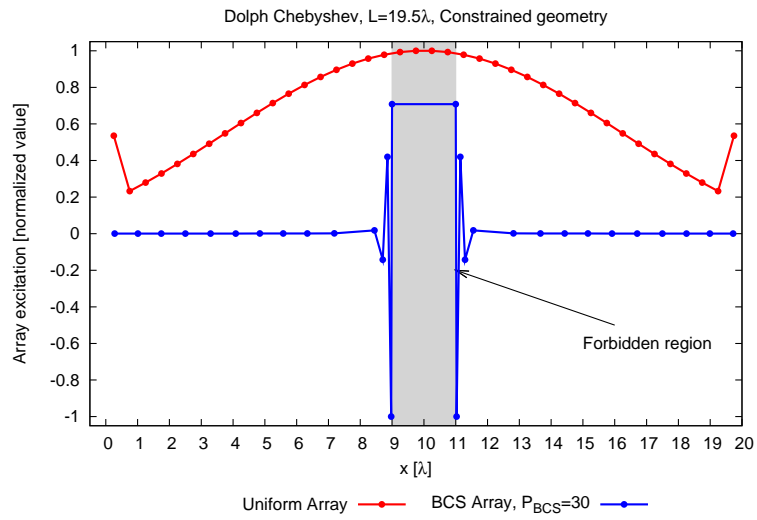


(a)

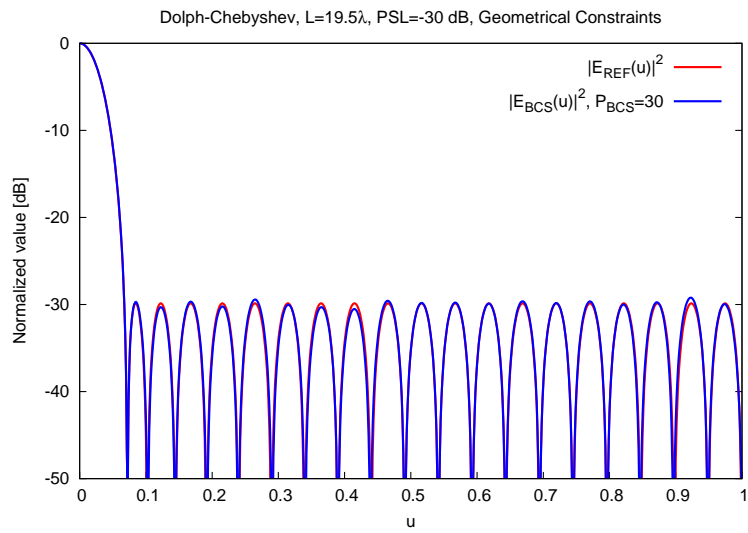


(b)

Figure 12 - G. Oliveri et al., “Bayesian Compressive Sampling for..”



(a)



(b)

Figure 13 - G. Oliveri et al., “Bayesian Compressive Sampling for..”

Table I - G. Oliveri et al., "Bayesian Compressive Sampling for..."

Reference Pattern			Uniform		BCS					
Type	L [λ]	PSL [dB]	P_{UNI}	$\frac{L_{UNI}}{L}$	ξ [$\times 10^{-5}$]	$\frac{P_{BCS}}{P_{UNI}}$	$\frac{\Delta L_{min}}{\lambda/2}$	$\frac{\Delta L}{\lambda/2}$	$\frac{L_{BCS}}{L}$	t [$\times 10^{-1}$ s]
<i>Dolph</i>	9.5	-30	20	1.0	2.62	0.70	1.26	1.46	1.000	1.12
<i>Dolph</i>	14.5	-30	30	1.0	9.98	0.66	1.35	1.52	1.000	2.93
<i>Dolph</i>	19.5	-20	40	1.0	7.10	0.65	1.50	1.56	0.997	2.14
<i>Dolph</i>	19.5	-30	40	1.0	3.03	0.70	0.78	1.42	0.995	1.18
<i>Dolph</i>	19.5	-40	40	1.0	9.09	0.65	1.56	1.56	1.000	1.13
<i>Taylor</i>	9.5	-30	20	1.0	7.82	0.70	1.22	1.46	1.000	1.27
<i>Taylor</i>	14.5	-30	30	1.0	9.64	0.66	1.35	1.52	1.000	3.14
<i>Taylor</i>	19.5	-20	40	1.0	8.53	0.65	1.34	1.55	0.994	1.92
<i>Taylor</i>	19.5	-30	40	1.0	3.13	0.65	0.80	1.43	0.993	1.48
<i>Taylor</i>	19.5	-40	40	1.0	3.62	0.65	1.36	1.54	0.990	1.01

<i>Reference Pattern</i>		<i>Method</i>	<i>Indexes</i>					
L [λ]	PSL [dB]		ξ	P	$\frac{\Delta L_{\min}}{\Delta L_{UNI}}$	$\frac{\Delta L}{\Delta L_{UNI}}$	$\frac{L}{L_{UNI}}$	t [s]
5.4	-20	[36]	—	10	1.00	1.00	1.00	—
5.4	-20	<i>BCS</i>	4.55×10^{-6}	10	0.34	0.96	0.96	1.5×10^{-1}
5.4	-20	<i>MPM</i>	7.82×10^{-3}	10	0.99	1.74	1.74	3.3×10^{-2}
5.4	-30	[36]	—	10	1.00	1.00	1.00	—
5.4	-30	<i>BCS</i>	8.27×10^{-6}	10	0.39	0.96	0.96	1.4×10^{-1}
5.4	-30	<i>MPM</i>	3.45×10^{-3}	10	0.99	1.74	1.74	2.5×10^{-2}
5.4	-40	[36]	—	10	1.00	1.00	1.00	—
5.4	-40	<i>BCS</i>	3.53×10^{-6}	10	0.63	0.97	0.97	1.6×10^{-1}
5.4	-40	<i>MPM</i>	0.84×10^{-3}	10	0.99	1.74	1.74	2.9×10^{-2}

Table II - G. Oliveri et al., “Bayesian Compressive Sampling for...”

	<i>Uniform</i>	<i>BCS</i>	<i>MPM</i>	<i>MPM</i> [37]
L [λ]	8.5	8.33	8.36	8.50
PSL [dB]	-20	-20.2	-13.2	-14.63
P	18	12	12	9
$\frac{P}{P_{UNI}}$	—	0.66	0.66	0.50
$\frac{\Delta L_{\min}}{\Delta L_{UNI}}$	—	1.18	< 0.01	1.42
$\frac{\Delta L}{\Delta L_{UNI}}$	—	1.51	1.52	2.12
$\frac{L}{L_{UNI}}$	—	0.980	0.984	1.00
t [s]	—	2.0×10^{-1}	2.8×10^{-1}	—
ξ	—	2.79×10^{-5}	4.02×10^{-3}	7.02×10^{-3}

Table III - G. Oliveri et al., “Bayesian Compressive Sampling for...”

	<i>Uniform (WLM)</i>	<i>BCS</i>	<i>MPM</i>
L [λ]	19.5	19.5	19.5
PSL [dB]	-17.2	-17.4	-3.6
P	40	26	26
$\frac{P}{P_{UNI}}$	—	0.65	0.65
$\frac{\Delta L_{min}}{\Delta L_{UNI}}$	—	0.975	< 0.01
$\frac{\Delta L}{\Delta L_{UNI}}$	—	1.56	1.56
$\frac{L}{L_{UNI}}$	—	1.0	1.0
t [s]	—	1.4×10^{-1}	3.3×10^{-1}
ξ		3.52×10^{-5}	4.81×10^{-2}

Table IV - G. Oliveri et al., “Bayesian Compressive Sampling for...”

Table V - G. Oliveri et al., "Bayesian Compressive Sampling for..."

<i>Reference Pattern</i>		<i>Constraint</i>	<i>BCS Indexes</i>					
L [λ]	PSL [dB]		ξ	P	ΔL_{min} [λ]	ΔL [λ]	L [λ]	t [$\times 10^{-1}$ s]
19.5	-30	$u_k \notin (0.5, 0.6)$	3.71×10^{-5}	26	0.455	0.776	19.36	2.17
19.5	-30	$u_k \notin (0.8, 1)$	6.81×10^{-5}	21	0.585	0.928	19.50	1.40
19.5	-30	$d_n \notin (5.3, 6.5)$ [λ]	5.82×10^{-6}	36	0.067	0.556	19.47	1.61
19.5	-30	$d_n \notin (0, 1)$ [λ]	4.81×10^{-5}	30	0.029	0.670	19.44	1.65